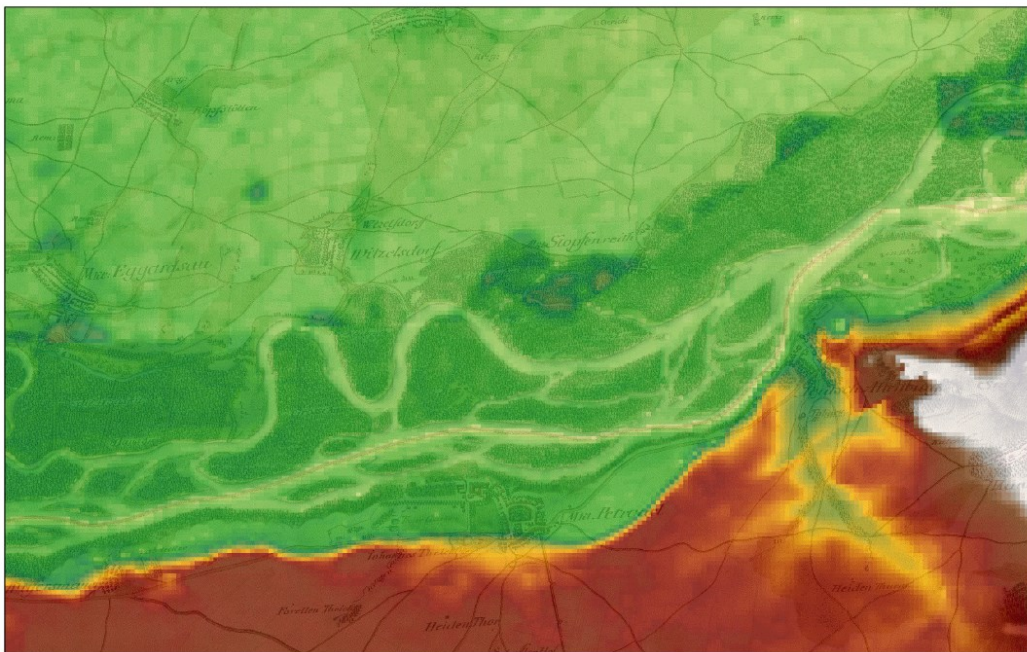


# An Evaluation of Flood Retention Capacity by the Danube Floodplains in Austria

Flood retention capacity is one of the ecosystem services provided by wetlands that is being progressively and globally degraded despite the increased number of environmental policies for the protection of natural resources (Millennium Ecosystem Assessment, 2005). The aim of this study is to develop and implement a methodology for evaluating flood retention capacity which could be applied to improve the decision-making process of river management strategies.

**Astrid Tishler**

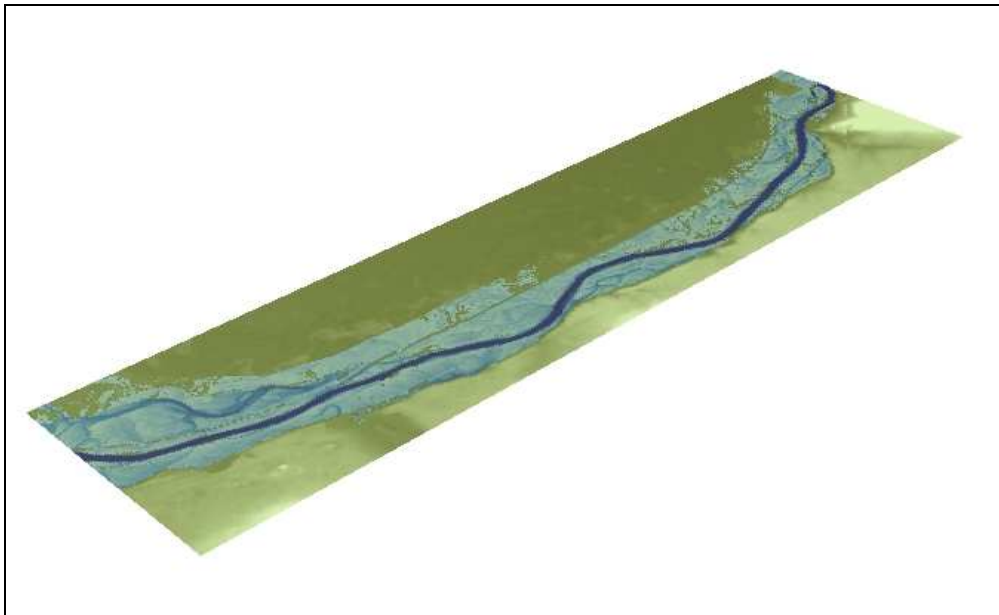


# **An Evaluation of Flood Retention Capacity by the Danube Floodplains in Austria**

MPhil Environmental Science  
Dissertation

By Astrid Tishler

Supervisor Prof. Keith Richards  
Word count: 15,082



August 2011



## Acknowledgments

I would like to thank my supervisor Prof. Keith Richards for all the advice and help that he has provided me during numerous discussions throughout the course of this study. Moreover, I would like to acknowledge Mr Christian Baumgartner from the Donau-Auen National Park, Mr Hannes Gabriel from Donau Consult and *via donau* for providing me the opportunity to study the Danube floodplains by enabling me access to data necessary for this thesis. The study was carried out under the Natural Environment Research Council studentship.

## Abstract

Flood retention capacity is one of the ecosystem services provided by wetlands that is being progressively and globally degraded despite the increased number of environmental policies for the protection of natural resources (Millennium Ecosystem Assessment, 2005). It has been established that in order to arrest the global degradation of wetlands' functionality, management strategies for natural resources should be refocused to consider the benefits of ecosystem service provisioning. The aim of this study is to develop and implement a methodology for evaluating flood retention capacity which could be applied to improve the decision-making process of river management strategies. The Donau-Auen National Park in Austria was used as a case study for the application of the methodology. Thus, the flood retention capacity was evaluated in both physical and monetary terms for the National Park area. The physical quantification applied a two-dimensional hydrodynamic model, Hydro2de, and a modified non-linear reservoir method for the calculation of flood storage volumes, residence times and average flood peak velocities of an annual, 30-year and 100-year flood event. For the economic evaluation, a substitute cost method was developed. In addition, the study developed a historical and future scenario, so that predictions could be made about how the service provisioning has and could change with time. The study estimated a maximum storage volume of 207 million m<sup>3</sup> by the total area which was valued to produce around 646,000 Euros of cost benefits in terms of flood protection. The historical flood retention capacity was found to have been smaller compared to current levels because of a higher floodplain discharge in the past. For the future, a small reduction in the flood retention capacity is predicted due to planned restoration programme that actually enhances floodplain flow. However, this will have no effect on the future value of the area as a mean of flood protection. The significance of these results is limited by the assumptions made in the study and hence, the calculated values can only be interpreted as an approximation for the study area in terms of flood retention provisioning. Furthermore, the implications are affected by the particular history of river morphology in the study reach and will not apply more generally.

## Table of Contents

Acknowledgments.....	2
Abstract.....	3
Table of Contents.....	4
List of Figures.....	5
List of Tables.....	6
1. Introduction.....	7
1.1. Background.....	7
1.2. Study area: Donau-Auen National Park.....	8
1.3. Aims and objectives.....	11
2. Methods.....	12
2.1. 2-D hydrodynamic model description: Hydro2de.....	12
2.2. Input data preparation for the Hydro2de model.....	13
2.2.1. Preparation of topography.....	13
2.2.2. Specification of boundaries.....	21
2.2.3 The specification of roughness: Manning's $n$ .....	22
2.3. Hydro2de parameterization.....	24
2.4. Calculating flood retention capacity in physical terms.....	25
2.4.1. Modified non-linear reservoir method.....	25
2.5. Past flood retention capacity.....	26
2.6. Future flood retention capacity.....	31
2.7. Economic Valuation: Substitute Cost Method.....	32
2.7.1. Step 1: Estimation of flood storage and a target group.....	32
2.7.2. Step 2: Alternative for flood water storage and its public demand.....	33
2.7.3. Step 3: Cost of the service.....	33
3. Results.....	35
3.1. Hydro2de calibration.....	35
3.1.1. Hydro2de comparison against monitoring data.....	35
3.1.2. Hydro2de comparison with calibrated HEC-RAS results.....	37
3.2. Results of the modified non-linear reservoir method.....	41
3.2.1. Present flood retention capacity.....	41
3.2.2. Past flood retention capacity.....	45
3.2.3. Future flood retention capacity.....	49
3.3. Monetary Value.....	53
4. Discussion of the estimated flood retention capacity.....	54
4.1. Present scenario.....	54
4.2. Past scenario.....	54
4.3. Future scenario.....	55
4.4. Monetary value.....	55
4.5. Model limitations.....	56
5. Conclusion.....	58
References.....	60
Appendix A.....	65

## List of Figures

Figure 1. Map of the study area, Donau-Auen National Park. ....	9
Figure 2. Complete topography used to represent the study area that combines topographic data from LiDAR, Sonar and SRTM datasets. ....	15
Figure 3. Bathymetric data gaps. A section of the Danube floodplain demonstrating data gaps between the DTM and bathymetric datasets. ....	16
Figure 4. A section of the Danube main channel with bathymetric data overlying the DTM. ....	17
Figure 5. A section of the Danube demonstrating the result of the inverse distance weighted interpolation method used to create a continuous dataset for the floodplain topography. ....	18
Figure 6. A summary of results comparison with varying topographic resolution ....	20
Figure 7. The use of hydrographs for the estimation of flood storage volume, residence time and velocity of the flood wave peak. ....	26
Figure 8. Historical maps of the area now under the Donau-Auen National Park. ....	27
Figure 9. Modified DTM used in the Hydro2de model for representing the hypothetical topography of the historical floodplains. ....	30
Figure 10. Comparison of predicted and measured water levels in the main channel.	35
Figure 11. Comparison of predicted and measured maximum water levels of the 100 year flood for the main channel. ....	36
Figure 12. Comparison of predicted and measured maximum water levels of the 100 year flood for the floodplain. ....	37
Figure 13. HEC-RAS and Hydro2de comparison of predicted water levels for the steady state (a), annual (b), 30- year (c) and 100-year flood events (d). ....	39
Figure 14. HEC-RAS and Hydro2de comparison of predicted flow velocities for steady state (a), annual (b), 30-year (c) and 100-year flood event (d). ....	40
Figure 15. Flood simulation results for the present scenario. ....	42
Figure 16. Flood simulation results for the past scenario. ....	46
Figure 17. Flood simulation results for the future scenario. ....	50

## List of Tables

Table 1. The initial roughness values defined according to the Arcement and Schneider (1989) criteria and the equivalent parameters in their calibrated form.....	23
Table 2. Preparation of input files for modelling historical flood retention capacity..	28
Table 3. The preparation of data input files for predicting flood retention capacity after the Integrated River Engineering Programme (IREP) has been executed.....	31
Table 4. The estimation of flood retention capacity in monetary terms. ....	34
Table 5. Nash-Sutcliffe efficiencies (E) for quantifying the model fit to field data. ....	37
Table 6. Summary of results for the present flood retention capacity.. ....	41
Table 7. Summary of results for the estimated historical flood retention capacity.. ....	45
Table 8. Summary of results for the predicted future flood retention capacity.. ....	49
Table 9. Summary of the monetary evaluation results. ....	53
Table 10. Comparison of wetland values in terms of produced flood benefits within literature.. ....	56

# 1. Introduction

## 1.1. Background

Flood retention capacity can be defined as the natural ability of floodplains to store flood waters and detain the propagation of flood waves, i.e. it characterizes the functionality of a region as a buffer area for reducing flood magnitudes and flood hazard. Several authors have discussed the significance of floodplains for the transformation of a flood wave peak, with the maximum runoff of the event being reduced and elongated over time (e.g. Kotze, 2000 and Pithart *et al.*, 2003). Hence, flood retention capacity of an area provides one of the ecosystem services produced by natural fluvial systems that can have a significant economic benefit.

The Millennium Ecosystem Assessment (2005) determined that over the past 50 years wetland ecosystem services, including flood retention capacity, have degraded more rapidly than ever before, despite the globally increasing number of environmental policies. Flood retention capacity is controlled directly by changes in surface elevations, geometry, size and shape of floodplains, roughness, location in the catchment, water regime and permeability of the soil (Kotze, 2000). These controlling factors of the ecosystem service have been altered as a result of several anthropogenic activities, including the transformation of land cover, hydrologic modification, drainage, infilling, spread of infrastructure and the consequential pollution, salinization and eutrophication (Millennium Ecosystem Assessment, 2005). Therefore, it has been proposed that a new approach which addresses environmental impacts of anthropogenic activities from ecosystem services perspective should be developed in order to cease the progression of global environmental degradation (Millennium Ecosystem Assessment, 2005).

Moreover, Barbier *et al.* (1997) proposed that a major reason for excessive depletion of wetland ecosystem services is the failure to account adequately for their non-market values in river management strategies and development decisions. Hence, there is a need for the development of methodologies that would facilitate the evaluation of the significance of ecosystem services, like flood retention capacity, within wetland management decisions. This would involve the quantification of the service in physical terms and for a more effective discourse with policy makers, planners and managers, the values of ecosystems may also be expressed in monetary terms.

Methods for quantifying flood retention capacity in physical terms have previously involved: (1) either hydrological flow routing or hydrodynamic models for calculating flow characteristics over the study area (i.e. water depths, velocities, discharge, area under water) and (2) non-linear reservoir methods or linear relationships for estimating the retained flood water volume and the speed of a flood wave (Valentova *et al.*, 2010). These methods have also enabled the evaluation of the effects of change in several factors identified by Kotze (2000) that control the provisioning of the service. Examples of assessing flood retention volumes with flow routing models include Ogawa and Male (1986) and Szolgay and Danacova (2008). These methods are applicable for river reaches where limited input data for hydrologic models is available in terms of surface elevations and the roughness of the study area. However,



the accuracy of the approach is limited by the representation of flow dynamics and geometric description (Valentova *et al.*, 2010). The application of the alternative approach, hydraulic models can be divided into 1-D (e.g. Miroslaw-Swiatek *et al.*, 2003; Sartor, 2005) and 2-D studies (e.g. Fukuoka and Watanabe, 2002; Valentova *et al.*, 2010). 1-D models require the adoption of major simplifications in process representation due to the fact that overbank flow cannot be modelled realistically and thus, has to be treated as flow through a separate channel (Miroslaw-Swiatek, 2003). Hence, 2-D hydrodynamic models provide an improved accuracy for process representation and for modelling floodplain flows within sub-channels (Connell *et al.*, 2001), and therefore are more appropriate for quantifying the flood retention capacity of floodplains. However, very few studies have laid out a detailed description of the methods applied in the quantification of flood retention capacity by 2-D models or discussed their accuracy. Therefore, further research is needed to develop and assess the applicability of these methods for the physical quantification of flood retention capacity.

There are a few studies in environmental economics that have explored the quantification of natural flood storage in terms of its monetary value (a summary of examples is given by Schuyt and Brander, 2004). As flood retention is a non-marketable benefit that is in direct use (i.e. it cannot be bought or sold on a market), its value can be considered equivalent to the cost savings received from reduced flood damage and smaller expenditure for flood protection measures proportional to the amount of retained flood water. Thus, if the provisioning of flood retention would cease to exist or be significantly reduced, the downstream areas would need to compensate for that loss by building new physical flood protection measures, or flood damage will occur. This creates an effective monetary value for the ecosystem service (King and Mazzotta, 2000). Hence, flood retention capacity has been most commonly evaluated by damage cost avoided and substitute cost methods, described in more detail by King and Mazzotta (2000).

Very few studies have previously combined a detailed assessment of flood retention value in both physical and monetary terms, despite the fact that the physical evaluation is partly a prerequisite for a monetary assessment. Hence, there is a need to develop an integrated approach which would combine environmental science principles of physical quantification with environmental economics for evaluating the monetary value of flood retention provisioning by floodplains. In order to explore the estimation of flood retention capacity in physical and monetary terms further, a case study is needed on the basis of which hydrologic modelling and economic evaluation could be carried out.

## **1.2. Study area: Donau-Auen National Park**

The study area includes the Donau-Auen National Park in Austria that protects ecosystems in one of the last functional alluvial reaches of the Danube with an interactive river-floodplain system (Schiemer *et al.*, 1999). A brief description of the area, its history and future restoration programmes will be given here.

The national park extends from Vienna to the Slovakian border, covering approximately 45 km in length and 9,300 ha area wise (Nationalpark Donau-Auen,

2011). It includes one of the few remaining wetlands in Central Europe that provides habitats for a large number of endangered and endemic species (Nationalpark Donau-Auen, 2011) (Fig.1). Beside its flood retention capacity, the area also provides a number of other ecosystem services, including groundwater recharge, sediment and nutrient retention, water purification, biological produce (e.g. wood, fish, game etc), climate change buffering in the form of a carbon sink and cultural services like recreation and tourism (Schwarz, 2010).

The land cover types of the area include riparian hardwood and softwood forests (65%), meadows (15%) and approximately 20% of the territory is under water during the mean flow conditions (Cierjacks *et al.*, 2010). Hence, the area is rich in the variety of habitats it provides. For example beside the main riverbed, the river-floodplain system accommodates oxbow lakes, side arms, steep riverbanks, gravel shorelines, riparian forests, meadows and xeric areas (Cierjacks *et al.*, 2010).

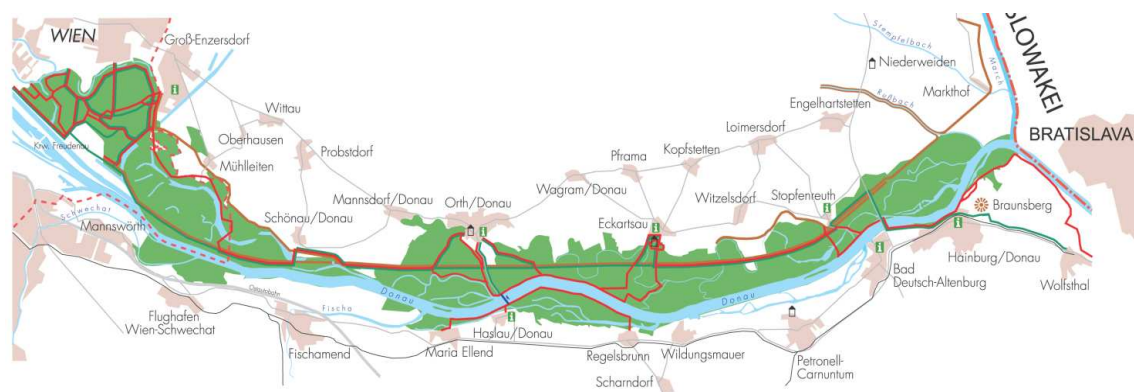


*Figure 1. Map of the study area, Donau-Auen National Park. The area is situated between two European capitals, Vienna (upstream) and Bratislava (downstream). The Danube reach passing through the National Park extends from the 1918.6<sup>th</sup> to 1885.6<sup>th</sup> river kilometres of the Danube.*

Hundreds of years of flow regulation works upstream and within the area have heavily influenced the ecosystem services sustained by the dynamic river floodplain system of the National Park, including the flood prevention capacity of the Danube floodplains. Since 1600s, the Austrian Danube has been continuously subject to flow regulation works for improving its navigational purpose, preventing channel migration, bank erosion and developing flood protection (Mohilla and Michlmayr, 1996; Hohensinner and Drescher, 2008). However, the first major flow regulation works started in Vienna in 1869 and since 1900s, the flood protection system of the Danube has been gradually improved for local urban developments (Mohilla and Michlmayr, 1996). All of this has resulted in fundamental changes to river geomorphology and hydrology as over the past few hundred years the naturally braided river of Danube has been transformed into a straight artificial channel in its reach through Vienna. The historical fluvial dynamics of the Upper Danube have been described by Hohensinner and Drescher (2008) and hence, the details of the past river-floodplain system from which the change has occurred will not be further discussed here.

As an overall result of the regulation works, the floodplains have been disconnected from the main Danube riverbed, with an exchange of matter occurring only during short term flood pulses (Tockner *et al.*, 1998). Up to 80% of former floodplain areas,

backwaters and side arms have been lost (Keckeis and Schiemer, 2002) owing to the fact that the main channel of the Danube has lowered approximately 1.5 m since 1875, causing a gradual dewatering of the floodplains and terrestrialisation of the backwaters (Schiemer *et al.*, 1999). Moreover, the Marchfeld dike built for flood protection cut off a large proportion of the natural floodplain area from the fluvial system. The intensity of geomorphological processes driving channel migration has also reduced while erosion has concentrated along the main channel of the river (Schiemer *et al.*, 1999). Other immediate effects of the completed flow regulation schemes include the loss of riverine inshore habitats and a reduced rate of groundwater recharge (Schiemer *et al.*, 1999; Keckeis and Schiemer, 2002).

Therefore, the regulation works have affected the natural functioning of the river-floodplain ecosystem, while the total effect on ecosystem services that the system provides remains unquantified. However, the semi-natural area of the Danube between Vienna and Bratislava still sustains some ecosystem functions characteristic to natural river-floodplain systems, although further research is needed into evaluating their current functionality. With the establishment of the Donau-Auen National Park in 1996, a restoration programme of the Danube floodplains was initiated for restoring its hydrological connectivity and both benefiting the endangered habitats and the navigational purpose of the river. The main goals of the restoration scheme included the promotion of floodplain habitats, reduction of bed scour in the main channel and sediment accumulation on the floodplain. Therefore, the restoration programme is expected to produce benefits in terms of natural ecosystem functioning and thus, service provisioning.

In order to provide a context for the benefits of the restoration programme in terms of ecosystem functioning, a few examples will be studied in more detail. For instance, a pilot project for the restoration programme was initiated between Haslau and Regelsbrunn in 1997 (Schiemer *et al.*, 1999). The side arm system was reactivated by lowering parts of the river embankment to the mean water level, creating artificial openings into the backwater system and lowering weirs from the main riverbed for a more continuous flow (Tockner and Schiemer, 1997; Schiemer *et al.*, 1999). As a result, the height of the river bed and the thickness of the fine sediment layer grew due to enhanced lateral erosion and the hydrological features became more heterogeneous. In addition, an increase in geomorphological processes was observed along with an induced length of the river shoreline and enhanced number of shallow water habitats.

Thereafter, the side arm systems have been reactivated similarly at Schönau and Orth. Moreover at Witzelsdorf and Hainburg, pilot projects for removing the artificial river embankments have been carried out. Tockner *et al.* (1998) listed three main hydrological outcomes for the restoration of the described side arm system: firstly an increase in the floodplain discharge, secondly an increased time of lotic conditions in the side arm system, and thirdly, a higher groundwater level. Furthermore, the changes in the hydrology reduced the bottom riverbed erosion due to diversion of flow (Tockner *et al.*, 1998). This demonstrates the significant potential of the restoration programme to affect the provisioning of several ecosystem services.

Currently, preparation works for a large scale restoration scheme, the Integrated River Engineering Project (IREP), are carried out. The scheme covers five main goals: (1) stopping river bed degradation by granulometric bed improvement (i.e. the addition of

450kg/m<sup>2</sup> of gravel to the main channel), (2) improving the navigational purpose of the river by applying a low flow regulation, (3) enhancing the fluvial dynamics of the river, (4) improving the hydrological connectivity between the river and the floodplains by further side arm reconnection and removal of artificial structures (embankments, weirs etc), (5) reducing water levels during flood events by reactivating the side arm system (Reckendorfer *et al.*, 2005). The IREP is currently at the stage of an Environmental Impact Assessment.

### **1.3. Aims and objectives**

The aim of this study is to improve the estimate of the flood retention capacity service provided by the Donau-Auen National Park in physical and monetary terms while also revising an appropriate methodology for the assessment with the combination of physical science and economics principles. The study will aim to develop a detailed record of the methodology with a discussion of the reasoning used for adopting the chosen techniques, something that the majority of related studies lack in detail.

The functionality of the ecosystem service will be assessed by estimating the stored flood water volume, residence time and the speed of flood peak propagation for an annual, 30-year and 100-year flood wave. These physical characteristics will be calculated on the basis of (1) outflow discharge estimates previously determined by unsteady flow simulations of a 2-D hydrodynamic model (Hydro2de) and (2) a modified non-linear reservoir method that analyses the inflow-outflow hydrographs. The first objective however is to run the Hydro2de model experimentally and compare its results against monitoring data and HEC-RAS predictions from a previous study (Donau Consult, 2006), so that the model could be parameterized to produce reasonable flow results for the current floodplain topography. Thereafter, the annual, 30-year and 100-year flood events will be simulated to produce outflow hydrographs and finally, the modified non-linear reservoir method will be applied to calculate the flood retention capacity of the study area in physical terms. Moreover, artificial scenarios where no overbank flow occurs will be simulated so that the total effect of floodplains on the propagation of the flood wave could be assessed.

The monetary evaluation will aim to account for the total economic contribution, i.e. the net benefits of the National Park that it provides as a flood protection instrument for downstream areas. Hence, the assessment will aim to quantify by a substitute cost method how much more would have to be spent on flood protection measures if the floodplains would cease to exist.

Beside the present condition of the ecosystem service provisioning, the study will aim to analyse how the production of flood retention has changed over the years as a result of past river management strategies. This assessment will be based on the analysis of historical maps and the modification of input topography in order to reflect changes in the geometry of the floodplain. In addition, a second modified input topography will be produced on the basis of scheduled works for the Integrated River Engineering Programme, so that an estimation of the future flood retention capacity could be made.

## 2. Methods

### 2.1. 2-D hydrodynamic model description: Hydro2de

The outflow hydrographs used for the quantification of flood retention capacity in physical terms were determined on the basis of flow modelling across the study area by a 2-D hydrodynamic model, Hydro2de. The model is based on the conservative form of depth averaged shallow water equations (Equations 1, 2, 3), while turbulence is represented by the zero-equation turbulence model and the numerical solution is reached via the finite volume method with explicit time integration.

Equation 1: (Conservation of mass)

$$\frac{\partial h}{\partial t} + \frac{\partial q}{\partial x} + \frac{\partial r}{\partial y} = 0$$

Equation 2: (Conservation of momentum in the x-direction)

$$\frac{\partial q}{\partial t} + \frac{\partial(q^2/h)}{\partial x} + \frac{\partial(qr/h)}{\partial y} + \frac{g}{2} \frac{\partial(h^2)}{\partial x} + gh \frac{\partial z}{\partial x} - \frac{1}{\rho} \frac{\partial(h\tau_{xy})}{\partial y} - \frac{1}{\rho} \frac{\partial(h\tau_{xx})}{\partial x} + \frac{\tau_{bx}}{\rho} = 0$$

Equation 3: (Conservation of momentum in the y-direction)

$$\frac{\partial r}{\partial t} + \frac{\partial(r^2/h)}{\partial y} + \frac{\partial(qr/h)}{\partial x} + \frac{g}{2} \frac{\partial(h^2)}{\partial y} + gh \frac{\partial z}{\partial y} - \frac{1}{\rho} \frac{\partial(h\tau_{yx})}{\partial x} - \frac{1}{\rho} \frac{\partial(h\tau_{yy})}{\partial y} + \frac{\tau_{by}}{\rho} = 0$$

Where h is the flow depth;

t is time;

q and r are units of discharge in x and y directions respectively;

g is the gravitational acceleration;

$\rho$  is fluid density;

$\tau_{xy}$ ,  $\tau_{xx}$ ,  $\tau_{yx}$  and  $\tau_{yy}$  are turbulent stresses from which  $\tau_{xx}$  and  $\tau_{yy}$  (normal stresses) are assumed to be negligible, while  $\tau_{xy}$  and  $\tau_{yx}$  (shear stresses) are calculated by applying the Boussinesq approximation;

$\tau_{bx}$  and  $\tau_{by}$  are the bed shear stresses that have been estimated by the quadratic friction law (Equations 4, 5).

Equation 4:

$$\tau_{bx} = \rho \gamma c_f u \sqrt{u^2 + v^2}$$

Equation 5:

$$\tau_{by} = \rho \gamma c_f v \sqrt{u^2 + v^2}$$

Where  $u$  and  $v$  are the velocity terms in  $x$  and  $y$  directions;  
 $c_f$  is the friction coefficient;  
 $\gamma$  is a factor accounting for the increased wetted area of sloping beds.

The friction coefficient,  $c_f$  is defined by Eq.6 which also demonstrates its relationship with Manning's  $n$ , the roughness coefficient.

Equation 6:

$$c_f = \frac{g n^2}{h^{1/3}}$$

The model uses two sets of rectangular uniform grids, the first containing surface elevations and the second roughness coefficients (Beffa and Connell, 2001). It applies initially dry floodplains in calculations unless specified otherwise, over which the flow is propagated on the basis of bed topography, difference in water levels, velocity and direction of flow (Beffa and Connell, 2001). The numerical flux from a cell is calculated by a flux difference splitting scheme developed by Roe (1981) which uses upstream weighting for estimating fluxes (i.e. an approximate Riemann solver). This approach is applicable for treating initially dry floodplains and allows the transition between sub- and supercritical flows (Nicholas and Mitchell, 2003). The second order accuracy of calculations is achieved by a variable extrapolation method (MUSCL approach) (Van Leer, 1977) which uses time steps determined by the Courant–Friedrichs–Lewy condition (Nicholas and Mitchell, 2003). Hence, Hydro2de is set to consider variable bed topography, processes of wetting and drying, bed friction and diagonal flows from grid cells (Beffa and Connell, 2001). Beffa and Connell (2001) describe the model in further detail.

Several authors have used Hydro2de for modelling floodplain flows and demonstrated its numerical stability (e.g. Connell *et al.*, 1998, 2001; Nicholas and Mitchell, 2003; Nicholas, 2003). However, it has been noted that Hydro2de may underestimate flow depths and the extent of a flood in the case of a low topographic resolution that ignores the distribution of some surface features (e.g. houses, hedges etc) (Connell *et al.*, 2001). Although this effect is also related to the specification of roughness, it has been determined that from input parameters, the topographic resolution affects the accuracy of predicted results the most (Connell *et al.*, 2001; Nicholas, 2003). Nicholas (2003) also emphasised that the monitored flow characteristics demonstrate more variability than the predicted results of the model, indicating a lack of sub-grid process representation by Hydro2de. Therefore, a special focus was adopted for preparing an input topography with the highest applicable accuracy.

## **2.2. Input data preparation for the Hydro2de model**

### **2.2.1. Preparation of topography**

The topographic data of the National Park used for model simulations originates from three surveys: airborne LiDAR survey with a resolution of 2.5 m, a Sonar dataset with a resolution of 2 m and SRTM data with a resolution of 90 m. The LiDAR data provided a representative DTM model of the National Park area with errors up to 40

cm as a result of laser scanning, filtering and data processing. The Sonar dataset described the bathymetry of the main Danube channel. Moreover, as Hydro2de can only process topographic input files in a rectangular shape, the rest of the topographic data within the rectangle around the area of interest formed by the LiDAR and Sonar data was interpolated from a SRTM dataset.

Figure 2 provides a full representation of the topography combined from the three datasets. The border between LiDAR and SRTM data, which were adjoined by a simple merge function, can be easily distinguished due to the difference in the original cell sizes of the datasets. However, the combination of LiDAR and Sonar datasets proved to be more complicated.

### **2.2.1.1. Topographic combination of LiDAR and Sonar data**

In order to construct a full topographic representation of the National Park area, two datasets (LiDAR and Sonar) had to be combined. However, a simple merge of the two raster datasets would create issues with the continuity of topography while the LiDAR data for the main channel area would be simply disregarded and replaced by bathymetric Sonar data. Firstly, as the bathymetric data were collected by a vessel travelling along the Danube, only a limited region of the channel could be accessed for gathering data due to groynes and islands on the river. Figure 3 demonstrates the bathymetric data gaps created by this limitation. Beside data gaps, a simple merging of two datasets would also generate abrupt jumps in topographic data on the border of the river and the floodplain to the extent of a few meters.

In order to overcome these issues, the following steps were taken:

- 1) The groynes and islands were digitized on the DTM as their location could be easily identified due to low water levels at the time of the LiDAR survey (Fig.4).
- 2) The DTM values of groyne and island surface elevations were transferred to the combined dataset.
- 3) Data gaps were eliminated on the basis of interpolation by inverse distance weighting (IDW) while using a power parameter 2, variable search radius and 12 points per radius (Fig.5). The method was chosen due to the relatively high accuracy and regular point data of the DTMs. Moreover, all the surrounding data points were assumed to have an equal weighting on the predicted elevations within the data gaps regardless of the direction of their location. Therefore, the IDW method provided a simple and convenient technique for interpolating values to the data gaps.



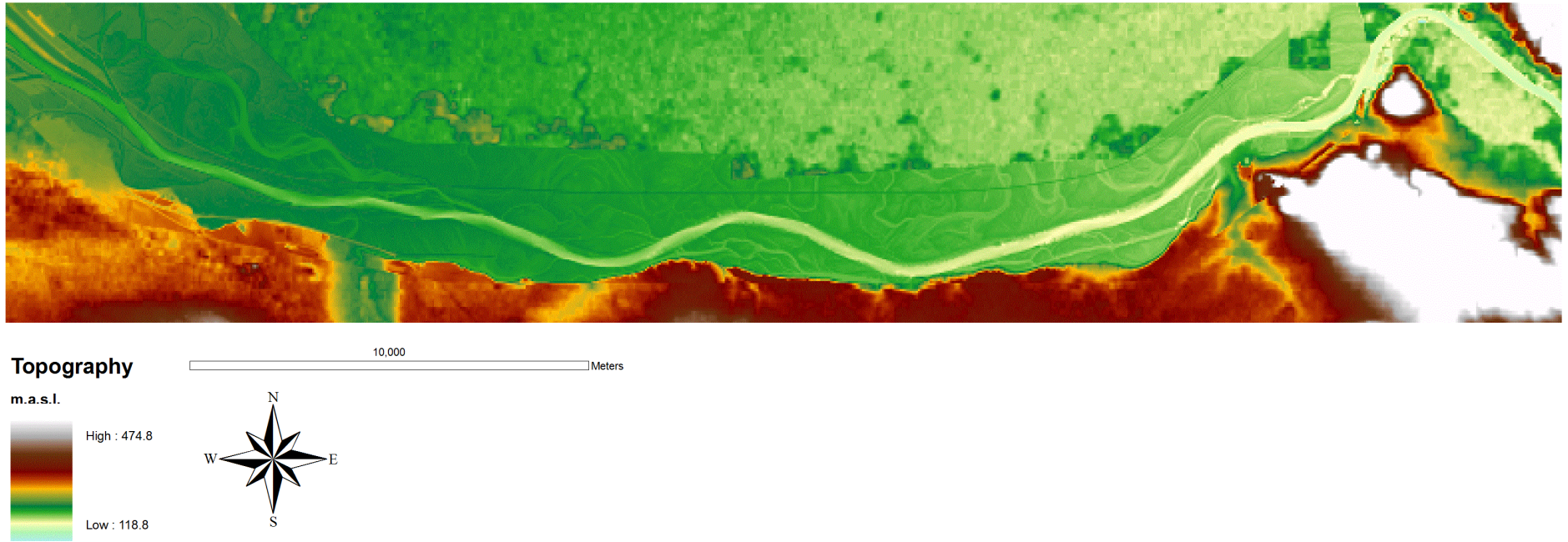
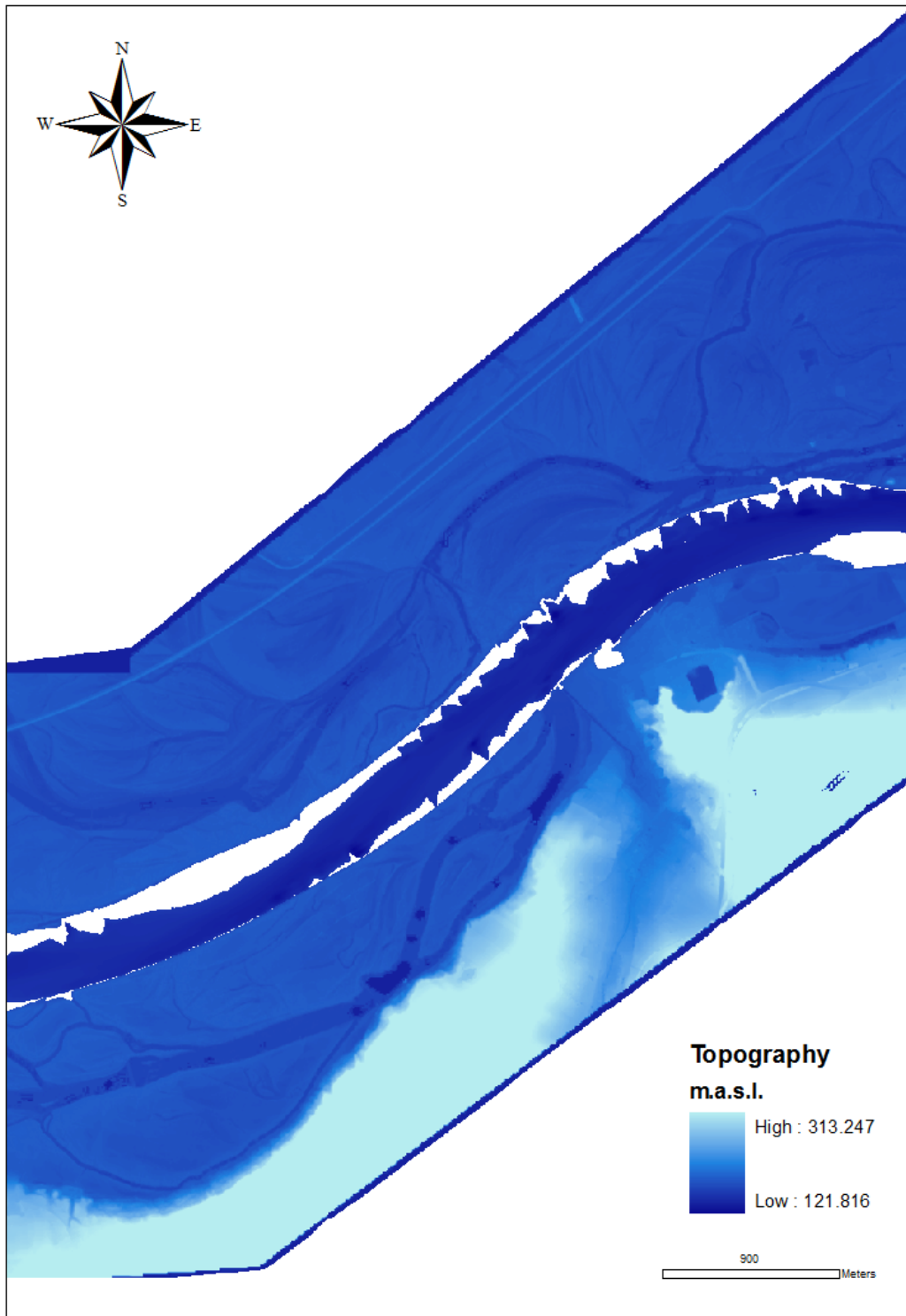


Figure 2. Complete topography used to represent the study area that combines topographic data from LiDAR, Sonar and SRTM datasets.





*Figure 3. Bathymetric data gaps.* A section of the Danube floodplain demonstrating data gaps between the DTM and bathymetric datasets. The continuous line on the Northern bank of the Danube represents the Marchfeld dike.

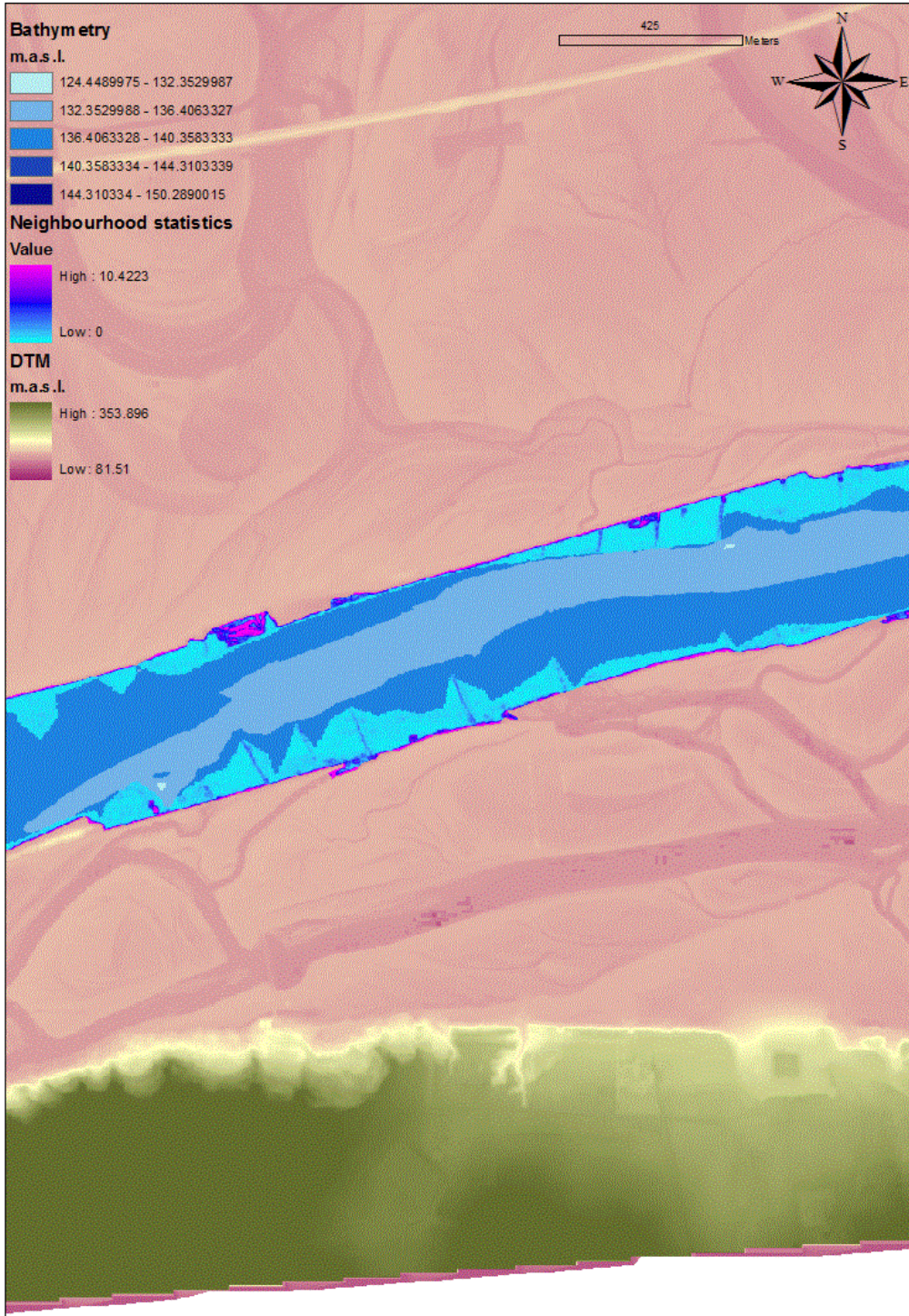
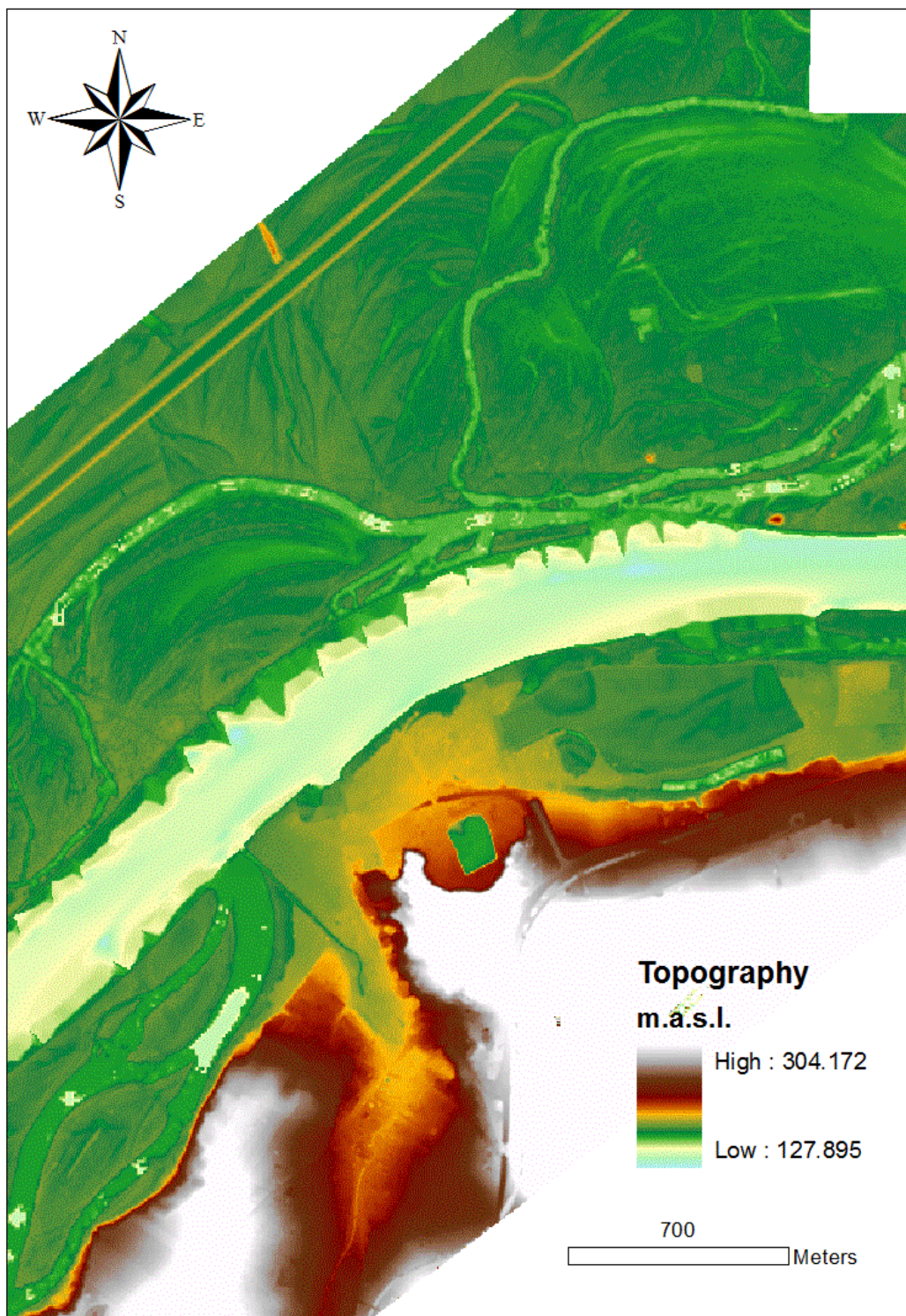


Figure 4. A section of the Danube main channel with bathymetric data overlaying the DTM. In the bathymetric data gaps of the river bed, the location and height of groynes and islands could be easily identified on the basis of neighbourhood statistics of the DTM as during the time of the LiDAR survey the water levels were below the groyne heights. The neighbourhood statistics signify surface elevations that are 1/3 of standard deviation times the value of the statistic different from surrounding elevations.





*Figure 5. A section of the Danube demonstrating the result of the inverse distance weighted interpolation method used to create a continuous dataset for the floodplain topography.*

### 2.2.1.2. Defining grid resolution

In order to find the optimum resolution for running model simulations, a number of test runs was carried out with different topographic resolutions, the results of which were thereafter compared and analysed. The maximum resolution with the smallest cell size that could be applied for the whole study area in Hydro2de was 15 m due to the limits set by the model for the size of the matrix that it can process. In addition, a number of more generalized resolutions, ranging from 20-100 m, was tested with an input discharge equivalent to a one-year flood event. The resolution of the topography was reduced by spatial averaging of surface elevations over a specific number of cells. As a result, the level of detail across the floodplain which generates flow intricacies was smoothed out. Because of the spatial averaging technique used, the traditional grid refinement analysis for calculating the Grid Convergence Index (GCI) (Roache, 1994), which estimates the convergence of a solution from the true numerical value, was not applicable for this study. For estimating GCI, grid resolution should be reduced by removing values from the mesh, e.g. every other value for resolution halving (Roache, 1997). However for the purposes of this study, it was important to generate an average representation of the topography which could later determine the general flow directions across the area.

Therefore in order to calculate how different the results produced by lower resolution topographies are, a percentage change of predicted depths and velocities from the 15 m resolution baseline was found (i.e. a fractional error from the 15 m resolution) with the assumption that the 15 m resolution topography would yield the highest accuracy for simulation results. Appendix A summarizes the statistics of the fractional errors from the 15 m resolution results relative to the increasing cell size, while Figure 6 provides a graphical representation of the key statistics in the results comparison.

Medians of fractional errors were used for the analysis as the occurrence of some extreme percentage changes skewed the mean values of the comparison and their equivalent standard deviations. The median percentage change decreased from -2.12% for 20 m resolution to -28.57% for 100 m resolution results, while the median percentage changes for velocities fell from 0.67% to -8.75% from 20 m to 100 m resolution respectively. Thus, the comparison showed that lowering topographic resolution decreases flow depths exponentially with an average of 0.34 % per 1% of resolution decrease according to the median values. Fractional errors in flow velocities demonstrated an increase in results until the 50 m resolution, after which further resolution reduction produced increasingly lower velocities than 15 m resolution. The average absolute change in velocities per 1% resolution decrease was 0.17%.

Hence, lower resolutions have a tendency to generally underestimate flow depths and also velocities at resolutions approximately three times smaller than that of 15 m. Connell *et al.* (2001) observed similar results and concluded that the underestimation occurs as the lower resolutions exclude important topographic detail that would otherwise increase flow depths. Nevertheless, some extreme percentage increases occurred for all comparisons as can be evidenced by the maximum fractional errors in Appendix A.

As the maximum percentage differences reached up to 186,700% for flow depths and 181,000% for velocities, the occurrence of outliers was analysed further in order to determine their significance on results with decreasing grid resolutions. The number of outliers for each set of comparison was determined while defining a value as an outlier if it satisfied conditions described by either Eq. 7 or Eq.8.

Equation 7:  $x < Q1 - 1.5IQR$

Equation 8:  $x > Q3 + 1.5IQR$

Where  $x$  is a value from the dataset to be determined as an outlier or non-outlier;

$Q1$  is the first quartile of the dataset;

$Q3$  is the third quartile of the dataset;

$IQR$  is the interquartile range.

Thereafter, the number of outliers was standardized according to the grid size. Within the dataset comparisons, roughly 8-11% of flow depths were significantly different from the results produced by the 15 m resolution topography (i.e. identified as outliers), while approximately 14-16% of flow velocities were significantly different (Fig.6). In addition, proportionally the number of outliers did not increase with lower resolutions, in fact it slightly decreased for fractional errors in flow velocities.

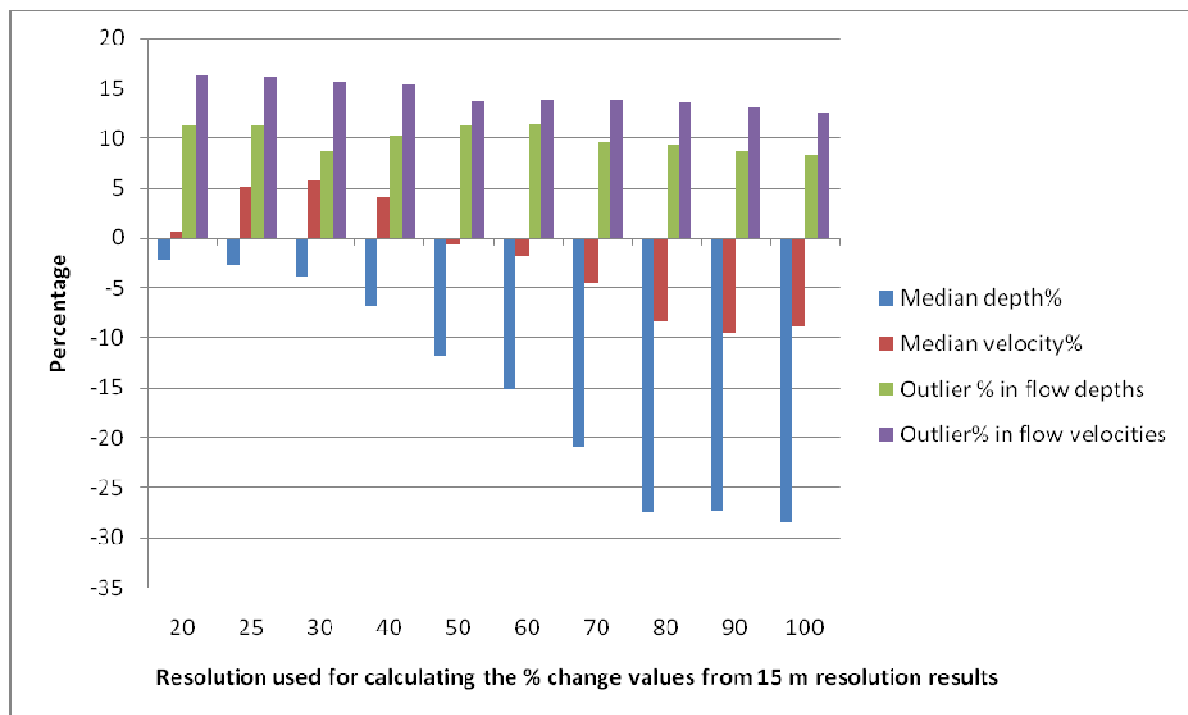


Figure 6. A summary of results comparison with varying topographic resolution. Median percentage changes of flow depths and velocities along with the percentage of outliers within the calculated fractional errors are demonstrated.

The majority of extreme percentage differences from the 15 m resolution results (i.e. outliers) occurred at the borders of side arms and the main channel. Hence, these were likely to be caused by the spatial averaging technique used to reduce the resolution of the topography. Spatial averaging smooths out the surface as a mean elevation value is assigned to an area that used to be covered by a number of smaller cells. When flow

is propagated over the smoothed surface, it is only to be expected that the main differences in flow characteristics while compared to higher resolution results will occur at locations where the higher resolution topography demonstrates a change in surface elevations but where the spatial averaging method has smoothed the features out on the lower resolution. These locations predominantly include the borders of the flow routes. The extreme differences are hence likely to occur when percentage change values are found from small depths or velocities at those borders.

As a result of the analysis, 50 m resolution topography was chosen for application in the rest of the simulations, based on three reasons. Firstly, the resolution demonstrated one the smallest fractional errors in predicted flow velocities while compared to the 15 m resolution. Secondly, the resolution produced an average level of percentage change in flow depths relative to the resolution increase. Thirdly, 50 m resolution enabled the running of simulations within a time frame available for this study, i.e. a 100 year flood simulation could be run in approximately 60 hours, 30 year flood event in 20 hours and an annual flood simulation in 8 hours. Considering that the study involved simulating each of the flood events 6 times (2 of each for the present, past and future scenarios), the total model running time added up to approximately 660 h while ignoring the time taken for test runs. Any additional resolution increase would have seen an exponential rise in the model running times.

### 2.2.2. Specification of boundaries

The outflow boundaries of the study area included the eastern and northern border of the region, while inflow was propagated from the western border. A terrace on the southern bank of the Danube prevented any outflow from that direction.

The eastern outflow boundary was specified with a slope of 0.01, i.e. as a boundary where flow is supercritical. The northern domain boundary was specified at a slope of 0.000001, so that if flow was to reach this border of the region, it could exit the study area, however any backwater or draw down effects would be minimal.

The western inflow boundary was specified according to field data. It was assumed that the modelled flood events were produced entirely by an incoming flood wave (characteristically flood events are caused in the area by the melting of Alpine snow and glacier ice) and that no precipitation occurs throughout the study area during the events. Thus, monitoring values of water levels from the Freudenua gauging station were used for the construction of a stage-discharge relationship. On the basis of this relationship and recorded water levels from the August 2002 floods, inflow hydrographs for the annual, 30- and 100-year floods were constructed. During the August 2002 floods, all three peak discharges of flood events in question were recorded and hence, the rising hydrograph values up to the relevant peak could be extracted from the dataset. However, the declining half of the hydrograph was partly extrapolated according to the recorded trend of decrease of the water level values. The slope for the inflow boundary was calculated from the constructed topography.

In addition, two small tributaries enter the Danube over the study region, however, their discharge is not continuously monitored. A HEC-RAS survey of the area (Donau Consult, 2006) estimated a discharge between 3-10 m<sup>3</sup>/s from both of the tributaries

depending on the water levels of the Danube which in comparison with the main channel discharge is negligible (respective main channel discharges varied from 900-10,400 m<sup>3</sup>/s). Therefore, for the purposes of this study the discharges from the tributaries were ignored.

### 2.2.3 The specification of roughness: Manning's $n$

In recent years, several studies have used remote sensing data for automated roughness parameterization of study areas in order to improve the accuracy of hydrodynamic modelling while classifying and clustering land cover types in terms of vegetation heights (e.g. Cobby *et al.*, 2001; Straatsma and Baptist, 2008; Casas *et al.*, 2010). These methods have improved the accuracy of modelling flow depths on floodplains up to the order of decimetres. However, the generation of a floodplain friction map requires the availability of several resources not accessible for this study, mainly in terms of time commitment and field validation.

Moreover, a number of difficulties arise with the specification of the roughness parameter. Beside representing friction, the value is also supposed to account for the limitations of the model, e.g. for processes not included. For example in this study among other processes, soil infiltration and evapotranspiration were ignored. Hence, the roughness parameter cannot be measured as such and needs to be calibrated on the basis of monitoring data.

The roughness parameter is also dependent on grid size as it accounts for the variation of surface elevations within the sub-grid resolution (Nicholas, 2005). Hence, topography provides an additional layer of data for describing the supra-grid roughness in terms of topographic variation. Nicholas and Mitchell (2003) distinguish between effective Manning's  $n$  and model  $n$  that are used in simulations. The effective  $n$  represents total roughness of the specified area that includes both the components of supra- and sub-grid scale. However for 2-D model simulations, a large proportion of the total roughness can be attributed to the model grid and hence, calibrated model  $n$  values which only aim to represent sub-grid scale roughness should be used. Thus, the calibrated values are dependent on the proportion of roughness that is already represented by the topographic grid.

Moreover for non-steady flows, the roughness parameter does not only vary spatially but also fluctuates with time as the value is dependent on the amount of submerged vegetation. As vegetation is covered by water, it bends and hence, the momentum-absorbing area is reduced along with the roughness coefficient (Wilson *et al.*, 2005). A decrease in roughness with increasing discharge has also been demonstrated by Nicholas and Mitchell (2003). Therefore, as the water levels rise during a flood event, the roughness of the area decreases and does not stay constant throughout the event. However, no temporal variation in the parameter can be expressed within the Hydro2de model.

Therefore while considering the issues discussed above, three roughness values were assigned for the study area on the basis of vegetation submergence as follows:

- 1) Main channel- the effects of vegetation were assumed to be negligible

- 2) Side arms- all vegetation was accounted to be submerged during an annual flood  
 3) Floodplain area and islands- emergent vegetation occurs during an annual flood

The three areas were defined as polygons as the channel boundary, islands, bankfull side arms and the floodplain area were digitized on the basis of the DTM and aerial photography. For side arms, only the channels that were inundated throughout the year were digitized as these are the areas where all occurring vegetation is submerged during high water levels.

The initial values of the Manning's  $n$  were assigned according to the roughness characterisation by Arcement and Schneider (1989) (Table 1). However bearing in mind the concepts of effective and model  $n$  as explained above, the roughness coefficients were calibrated to smaller values. The process of calibration is explained further in Section 2.3.

*Table 1. The initial roughness values defined according to the Arcement and Schneider (1989) criteria and the equivalent parameters in their calibrated form.*

Characteristic	Symbol	Description and estimated value		
		Main channel	Side arms	Floodplain and islands
Base value of the roughness coefficient relative to the median size of bed material	$n_{\text{base}}$	Coarse gravel 0.026	Sand channel, median sed. size 0.4 mm 0.02	Same as for sidearms 0.02
Degree of bank irregularity	$n_1$	Minor 0.004	Minor 0.005	Moderate (rises and dips) 0.01
Variation in channel cross-section	$n_2$	Alternating occasionally 0.005	Alternating occasionally 0.005	N/A
Effect of obstructions	$n_3$	Minor 0.005	Appreciable 0.02	Appreciable 0.03
Amount of vegetation	$n_4$	Small 0.01	Medium 0.015	Extreme 0.1
Channel meandering	$m$	Minor 1.0	Severe 1.3	N/A (1.0)
$n_{\text{total}} = (n_{\text{base}} + n_1 + n_2 + n_3 + n_4) \times m$	$n_{\text{total}}$	0.05	0.08	0.16
Calibrated value		0.05	0.06	0.07



### 2.3. Hydro2de parameterization

Two parameters were calibrated in order to find the best fit of model predictions with the observed field data. These included spatially distributed roughness parameters (Manning's  $n$ ) and the constant coefficient of eddy viscosity ( $cv$ ). Firstly, the values were calibrated against monitored water levels equivalent to a steady state flow simulation with an input discharge of  $1923 \text{ m}^3/\text{s}$  that represents the arithmetic mean of the long-term discharge record (*via donau*, 1996), i.e. the average flow discharge at the beginning of the reach. Secondly, an unsteady simulation, depicting the conditions of the 100-year flood that took place in August 2002, was run with a hot start from the previously calibrated steady state water levels. Thereafter, the 100-year flood water levels were calibrated against recorded field data for the maximum flood levels. The main channel and floodplain results were examined separately. Unfortunately, the parameters could not be calibrated against monitored annual and 30-year flood levels as no field data could be accessed for those events. In addition, no calibration data for distributed discharges or flow velocities were available for the study area.

Thus, the parameter calibration was carried out twice, firstly for the steady state and secondly for the unsteady state flow. It was assumed that the parameter values calibrated for the 100-year flood would also be applicable for other unsteady flow simulations, i.e. for the annual and 30-year flood, despite the fact that roughness and turbulence are dependent on discharge. During the course of calibration, it was determined that the effects of changing the turbulence coefficient were minimal (equivalent to an average change of  $0.00002 \text{ cm}$  in flow depths per 10% change in turbulence). On the other hand, a decrease in the roughness value of 10% caused the average reduction of flow depths of approximately  $0.017 \text{ cm}$ . More importantly however, changing these two parameter values also affected the distribution of water levels across the study area. Thus, the reduction or increase of the roughness and turbulence coefficients did not decrease/increase flow depths by the same amount throughout the region. Therefore during the calibration process, the results of both steady and unsteady simulations were fit to match the monitoring data by identifying parameter values that would produce the observed water level distributions. In order to reduce the remaining differences, model predictions were further multiplied by a constant which was chosen so that the average difference between monitored water levels and model predictions would be minimal.

The assumption was made that the water level distribution for the three flood events in question (annual, 30-year and 100-year floods) would remain a constant reflection of the topography of the floodplain. The change in the observed flood extent for the three flood events would be minimal because of the dike on the northern bank and the terrace on the southern bank that border the area available for overbank flow from the main channel. Therefore, the water level distribution would be proportional for all three flood events as the area would be flooded in a similar sequence while the height of water levels would change in response to the magnitude of the flood wave. Hence, it can be said that in order to keep the water level distribution proportional for all three flood events, the model parameters should remain at the level calibrated for one of the events as otherwise, bias in terms of water level distribution would be introduced. The height of the actual water level would, however, depend on the magnitude of the event, i.e. input discharge.

## **2.4. Calculating flood retention capacity in physical terms**

After the calibration of the Hydro2de model, the following steps were taken. Firstly, the Hydro2de model was run to equilibrium with a discharge of 1923 m<sup>3</sup>/s (i.e. the arithmetic mean discharge of the Danube at the upstream end), 50 m topographic resolution and calibrated parameter values (roughness and turbulence coefficients). Secondly, three unsteady flood events (annual, 30-year and 100-year floods) were propagated with a hot start from the steady state run. The outflow hydrographs at the downstream boundary were recorded along with flow depths, water levels and velocities for the whole mesh of each of the simulation. The outflow from the study area occurred across two boundaries, the eastern and northern edge of the region. Therefore, the total outflow hydrograph was calculated as the sum of discharges from both boundaries at each one hour time interval. These simulations will be referred to in the Section 3 of the study as “the total study area simulations” due to the fact that inflow was not restricted to the main channel and could freely propagate across the floodplains on the basis of the distribution of surface elevations.

In order to quantify the effect of floodplains on the flood retention capacity, a scenario where no flow enters the floodplains or side arms was constructed. The no-floodplain-flow scenario was generated by only including the main channel bed elevations within the topographic input file, thus, representing the flood retention capacity of the main channel alone. The difference between the total study area simulation and no-floodplain-flow scenario retention volumes of the three flood events indicates the total effect of floodplains on the provisioning of the ecosystem service.

### **2.4.1. Modified non-linear reservoir method**

The total flood retention capacity of the area was assessed on the basis of three terms: the volume of retained flood water, residence time of flood waters and the speed of the flood wave peak propagation during the event. Figure 7 along with Equations 9, 10 and 11 define the principles underlying the modified non-linear reservoir method used for the evaluation of the three variables. The total water volume stored on the floodplain during a flood event was calculated by finding the difference between the areas of inflow and outflow curves (Eq. 9), while the flood residence time was assumed to equal the time taken for the outflow to normalise to its steady state equivalent (Eq.10). Moreover flood wave celerity was found by calculating the difference in times as a fraction of the distance travelled between the inflow and outflow peaks (Eq. 11), thus representing the time it took for the peak of the flood wave to travel to the end of the study area.

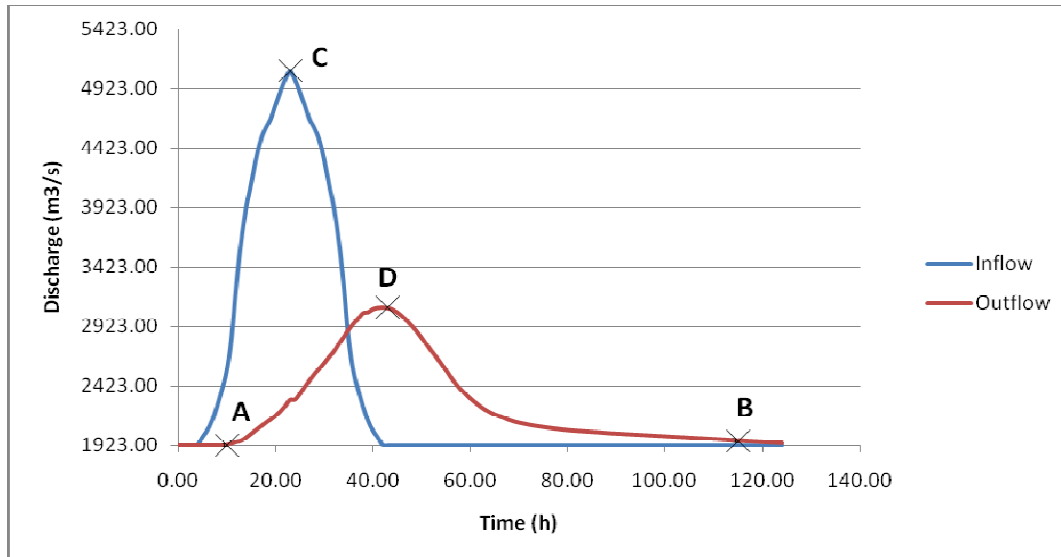


Figure 7. The use of hydrographs for the estimation of flood storage volume, residence time and velocity of the flood wave peak. The annual flood hydrographs were used for this example. The calculation of flood retention volume, residence time and flood wave celerity from the drawn hydrographs is defined by Equations 9, 10 and 11.

$$\text{Equation 9: } V = \sum [(Q_{in} - 1923) \times t] - \sum [(Q_{out} - 1923) \times t]$$

$$\text{Equation 10: } T = t_B - t_A$$

$$\text{Equation 11: } v = 39.05 / (t_D - t_C)$$

Where 39.05 is the length of the study area in km.

Equation 9 demonstrates that the inflow and outflow total water volumes were calculated as approximations of the areas under their equivalent curves, while the true values will be slightly larger than the estimations used in this study. It is also important to note that the base level value of 1923 m<sup>3</sup>/s was subtracted from all discharge readings (Eq.9) in order to account solely for the additional flow from a flood event.

## 2.5. Past flood retention capacity

Simulations predicting the past scenario aimed to depict the natural state of the floodplains unaffected by river regulation works and urban development, so that the results could indicate the maximum natural flood retention capacity of the floodplains. Major river regulation works started in Vienna in the 19<sup>th</sup> century, hence a set of historical maps from 1773-1781 was used as a baseline for representing the natural state of the river-floodplain system. Figure 8 provides an illustration of the scanned historical maps used in the study, while Table 2 summarizes the changes made to the input files. As an underlying assumption for the modification of the topographic input data, the current DTM of the area was considered to have preserved some features of

the historical topography. Figure 9 demonstrates the hypothetical historical topography produced as a result of the modifications listed in Table 2.

After the modification of input data to represent the historical floodplain conditions, four Hydro2de flow simulations (steady state, 100-year, 30-year and annual flood) were run with equivalent input discharges to the simulations from the present scenario. The flood retention volume, residence time and flood wave speed for each of the flood events were thereafter calculated according to Equations 9, 10 and 11. Similarly to the present scenario, a no-floodplain-flow topographic scenario was constructed with flow constricted only to the channel system. Thereafter, the resultant retention volumes from the no-floodplain-flow scenario were used to quantify the total effect of historical floodplains on the flood retention capacity by calculating their difference from the scenario where floodplain flow occurred.

#### Josephinische Landesaufnahme von Wien bis Hainburg (1773 - 1781)



*Figure 8. Historical maps of the area now under the Donau-Auen National Park. The hand-drawn maps originate from the first comprehensive military mapping project of the Habsburg hereditary lands and were constructed between 1773-1781.*

Table 2. Preparation of input files for modelling historical flood retention capacity.

<b>Change from historical conditions</b>	<b>Modification of input data</b>	<b>Issues/ Assumptions</b>
Topography: The construction of manmade structures for improving flood protection and navigation (e.g. embankments, dike, groynes)	1) The dike was digitized on the current DTM of the area, its surface elevations were extracted and recalculated by interpolation from nearby values using the inverse distance weighting (IDW) method. 2) Groynes and embankments were removed from the DTM along with the current main channel and side arms, their surface elevations were replaced by the IDW method as if no river channels existed.	Interpolation of surface elevations could lose topographic detail.
Topography: Changes in the distribution of channels	The historical braided channels of the Danube were digitized on the basis of historical maps and their polygons were transferred to the current DTM in order to account for the change in the distribution of channels.	The system used to be in a dynamic equilibrium with unstable banks and the location of side arms shifting regularly (Reckendorfer <i>et al.</i> , 2005), thus, any combination of the distribution of historical channels may be only representative of a very short time period.  The accuracy of the historical maps is unknown, therefore, some errors in the location and width of the channels may have occurred.
Topography: Depth of the historical channels	1) A point data layer representing an arbitrary depth of 3 m was distributed across the historical channel system on a coarse resolution.  2) Thalweg of the historical channel system was digitized on the basis of historical maps and transferred as a polygon to the DTM. The depth of the thalweg was recalculated as a whole while accounting for the fact that since 1875 water levels have lowered 1.5 m (Schiemer <i>et al.</i> , 1999). As	A uniform incision rate within the main channel throughout the 30 km long river reach is unlikely to be completely realistic. In addition, no information on actual river depths is available for the pre-1875 time period.

	<p>the current average maximum depth of the main channel is 8 m, the historical channel was assumed to have an average maximum depth of 6.5 m.</p> <p>3) The IDW method was used to produce a finer resolution topography and to interpolate between the thalweg, channel and floodplain surface elevations in order to create a smooth, continuous topography.</p>	
<p>Roughness: Changes in the distribution of the roughness coefficient due to changed land cover types and channel system.</p>	<p>1) The entire channel system was assigned the roughness value equivalent to the main channel of the present scenario, 0.05.</p> <p>2) The rest of the floodplain was assigned the roughness value equivalent to the current roughness of the floodplains, 0.07.</p>	<p>1) It was assumed that the sub-channels of the historical Danube were more similar to the current main channel in terms of the median bed sediment diameter and consequential roughness than to the side arms of the present scenario.</p> <p>2) The main changes in the floodplain roughness are produced by the distribution of softwood-hardwood forests and the increased flow area under the anabranching river channels (Hohensinner and Drescher, 2008). As the specification of roughness coefficient for the present scenario did not account for the differences in roughness of softwood and hardwood forests and represented an area with a similar forest to meadow ratio, it was assumed that the average roughness of the historical floodplain area not under water would be equivalent to the calibrated present scenario value.</p>



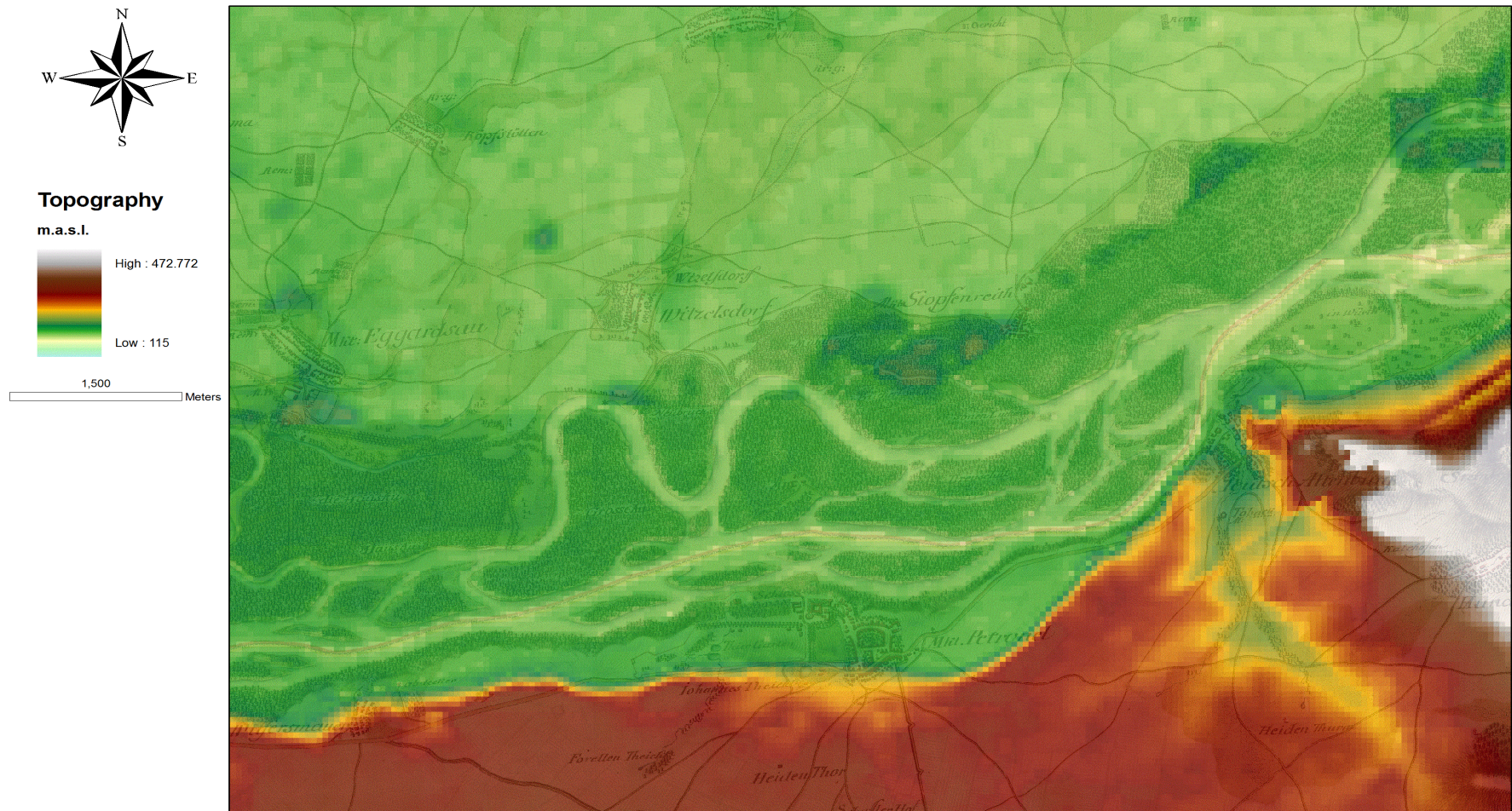


Figure 9. Modified DTM used in the Hydro2de model for representing the hypothetical topography of the historical floodplains.

## 2.6. Future flood retention capacity

The future scenario was developed to represent the area in approximately 50 years time with the assumption that all of the Integrated River Engineering Programme's (IREP) aims have been carried out by then across the National Park area. Thus, in order to predict the future flood retention capacity of the Donau-Auen National Park, the effects of the programme's objectives on factors controlling the provisioning of the service were analysed. Table 3 summarizes the objectives of the IREP that are likely to influence the flow dynamics and storage capacity of the floodplains and how these changes were reflected during the modification of input data to the Hydro2de model.

After the modification of input data, the steady state, 100-year, 30-year and annual flood events were run on Hydro2de and the characteristics of flood retention capacity (volume, residence time, flood wave speed) were calculated as described above (Equations 9, 10 and 11). In addition, a no-floodplain-flow scenario was constructed for the modified future topography and run on Hydro2de with the steady state flow and equivalent flood event discharges. The total predicted future effect of the floodplains on the retention capacity was thus calculated by finding the difference in retained water volumes between flood event scenarios with and without floodplain flow.

Table 3. The preparation of data input files for predicting flood retention capacity after the Integrated River Engineering Programme (IREP) has been executed.

IREP objective	Modification of input data	Issues/ Assumptions
Granulometric bed improvement by the addition of 450 kg/m <sup>2</sup> of gravel to the main channel (Reckendorfer <i>et al.</i> , 2005)	Main channel bed elevations were increased by 25 cm.	A uniform addition of gravel was assumed, although in practice an adaptive implementation strategy will be applied according to the local degradation tendency (Reckendorfer <i>et al.</i> , 2005).
Improvement of inlet structures to side-arms from the main channel by lowering cross dikes/ weirs (Schwarz, 2010)	The cross dikes at inlets between the main channel and side arms were lowered by 0.5 m.	It was assumed that all inlets of side arms would be improved for hydrological connectivity with a constant arbitrary depth decrease.
Removal of bank revetments/ steep artificial embankments and the widening of the river bed (Reckendorfer <i>et al.</i> , 2005; Schwarz, 2010)	Surface elevations within around 0.5 m from both sides of the main channel banks were extracted and replaced by the IDW method in order to remove the steep artificial embankments and to create a smoother topography.	A uniform reduction in the bank steepness of the Danube was assumed throughout the study area.



## **2.7. Economic Valuation: Substitute Cost Method**

The economic evaluation of flood retention capacity by a substitute cost method involved the execution of three steps: (1) quantifying the levels of the ecosystem service provided in physical terms for the identified target consumer group; (2) identifying the cheapest alternative for the provisioning of the service and establishing a public demand for it; (3) calculating the cost of the service on the basis of substitute costs (King and Mazzotta, 2000).

The substitute cost method was chosen as the preferred evaluation approach for economic analysis due to the following reasons. Firstly, the substitute cost method is unaffected by the probability of the flood events, hence, simplifying the assessment process (Bouma *et al.*, 2005). Secondly, the data necessary for this analysis is readily accessible which is not the case for quantifying damage costs from flood events in the study area, one of the alternative methods for economic evaluation. Thirdly, the approach does not require the application of extensive resources and hence, can be carried out quickly.

### **2.7.1. Step 1: Estimation of flood storage and a target group**

As a general rule, flood protection structures are built to withhold the flood waters of an event with a recurrence interval of 100 years. Therefore, the predicted hydrographs of the 100- year flood event for the present, past and future scenarios were used in the economic evaluation. The difference between the total outflow volume of the total study area and no-floodplain-flow scenarios was assumed to represent the increase in water volumes received during a 100-year flood event if no flood retention service was provided by the floodplains of the National Park.

The target consumer group was identified as the population of Bratislava (around 500,000 inhabitants), the first suburbs (Devin and Devinska Nova Ves) of which are situated approximately 1 km downstream from the border of the total combined study area and are the first urban areas to receive the flood waters of the Danube after it has passed through the Donau-Auen National Park. Two major assumptions were made while defining Bratislava as the target group. Firstly, it was assumed that the 1 km stretch between the study area and Bratislava suburbs would not act as a major buffer area and thus, the changes in discharge while comparing the total floodplain and no-floodplain-flow scenarios would be directly propagated to the target group. Secondly, the effects of inflow from the Morava tributary were ignored for the simplification of the assessment with the assumption that the additional inflow from the tributary would not change the difference in received flood water volumes between the total study area and no-floodplain-flow scenarios.

Therefore if no flood retention service was provided by the floodplains, the 100-year flood water volumes that Bratislava receives would be equivalent to the sum of the current flood volumes and the difference between the outflow volumes of the total floodplain and no-floodplain-flow scenarios.

### **2.7.2. Step 2: Alternative for flood water storage and its public demand**

The manmade flood protection structures of Bratislava were considered to be the alternatives for the flood water storage on the floodplains. For example, an extensive flood protection project for Bratislava that reconstructed the flood protection structures of the city was recently finished. It included the construction of 13 km of flood protection along the Danube and 5 km along the Morava tributary, the reconstruction and strengthening of existing dikes, establishing of pumping stations, purchasing of monitoring equipment etc (Hirnerova and Sabo, 2010; ICPDR, 2010). The total cost of the project was approximately 31 million Euros (Liptak, 2007; Sabacek, 2011).

For the purposes of this study, it was assumed that the total level of investment made for the prevention of flood damage in Bratislava will provide sufficient flood protection to withhold any major economic loss from a 100-year flood event. Moreover, it was assumed that the cheapest options were used for delivering the required level of quality and quantity in flood protection. Therefore, the current flood protection value to protect against a 100-year flood event (i.e. 10,320 m<sup>3</sup>/s peak discharge) is approximately 31 million Euros. It was assumed that the flood protection structures will hold this level of value annually because of yearly repairs and extra investment to conserve the overall value of the system, even if the actual value of construction and equipment depreciates over time with reduced functionality. Thus, it can be said that the value of the established flood protection is 31 million Euros per year.

The public demand for the service is established by the construction of extra flood protection structures in order to avoid economic losses from flood hazard. In essence, it is cheaper to invest in flood protection than to pay for flood damage, this creates a demand for establishing flood protection measures.

### **2.7.3. Step 3: Cost of the service**

The value of the flood storage capacity of floodplains was calculated on the basis of a simple ratio between the costs associated with the current level of the total 100- year flood volume and the expected costs associated with a hypothetical 100- year flood event equivalent if no flood storage was provided by the Donau-Auen National Park (Table 4). Therefore, the costs of the additional flood protection structures needed, if no flood storage by the floodplains existed, were treated as a marginal cost from the previous total investment, assuming a linear relationship. The difference between the estimated costs and current costs were assumed to represent the value of the Donau-Auen National Park as a mean of flood protection. The concept has been schematically illustrated in Table 4.

Table 4. The estimation of flood retention capacity in monetary terms.

Volumes of flood waters received by Bratislava during a 100-year flood event (m <sup>3</sup> )	Cost of equivalent flood protection (mil. Euros per year)
<b>V<sub>1</sub> (total outflow volume calculated for the total study area scenario of the present situation)</b>	31
<b>V<sub>2</sub> (total outflow volume calculated for the no-floodplain-flow scenario)</b>	$C = 31(V_2 / V_1)$
<b>Total value= C-31</b>	

## 3. Results

### 3.1. Hydro2de calibration

#### 3.1.1. Hydro2de comparison against monitoring data

Figure 10 demonstrates the good compliance of predicted steady state and measured water levels in the main channel achieved as a result of model parameterisation. The model bias, process representation and precision of the Hydro2de predictions can be described by the slope, intercept and  $r^2$  value of linear regression analysis respectively (Lane *et al.*, 2005). If the model results comply perfectly with field data, the slope and  $r^2$  value of the trend line would be equal to 1 and the intercept would be equal to zero (demonstrated by the blue dashed line on Fig.10) (Flavelle, 1992). Hence, calibration of model parameters was used to optimize the fit of the trend line to the 1:1 agreement line as shown on Fig.10.

As the slope and  $r^2$  values were approaching unity, it can be said that model bias was small and precision relatively high. The intercept of 3.6218 was not considered to be problematic, however. The water levels are in meters above sea level, thus, extrapolating back to zero is a long way from the real data and a very slight deviation of the gradient from 1 would result in a rather large intercept.

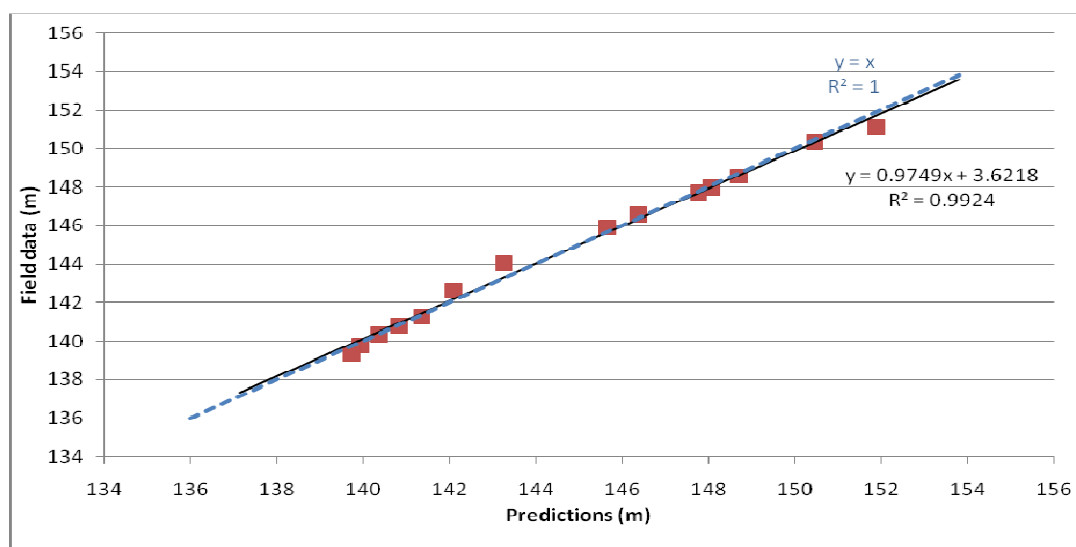


Figure 10. Comparison of predicted and measured water levels in the main channel. The blue dashed line represents the perfect 1:1 agreement of model results and field data. The solid line is the regression line of the actual comparison between field data and calibrated model predictions.

Similarly, model compliance with the monitored maximum 100-year flood water levels for the main channel and floodplain was evaluated according to the field observation records provided by *via donau*, the Danube waterway management company. Floodplain water levels were calibrated against 20 data points measured nearby the dike while the main channel monitoring data was collected from six locations along the Danube on 15 August 2002. Figures 11 and 12 demonstrate the fit of model predictions with the main channel and floodplain monitoring data respectively.

After parameter calibration, strong compliance of model predictions and measured 100-year flood field data was achieved for the main channel water levels as can be evidenced from the slope and  $r^2$  values that are approaching the value 1 (Fig.11). In addition, the intercept indicates that the model has included the majority of flow processes that control the height of water levels. However, some imprecision of model calculations can be seen by the scatter around the regression line which was likely to have been produced by either uncertain input data and/or errors in the monitoring data (Flavelle, 1995).

Model compliance with monitored water levels of the 100- year flood event across the floodplain was not as strong even after parameter calibration (Fig.12). The comparison indicates imprecise input and/or field data, poor process representation by the model and bias in model results as can be evidenced from the  $r^2$  value (scatter around the trend line), large intercept and the slope respectively. The inaccuracies were likely to have been produced by an insufficient precision in determining the distribution and value of the roughness coefficients. In addition, the resolution of input topography could have influenced flow routing over the floodplains due to its reduced detail in the distribution of surface elevations.

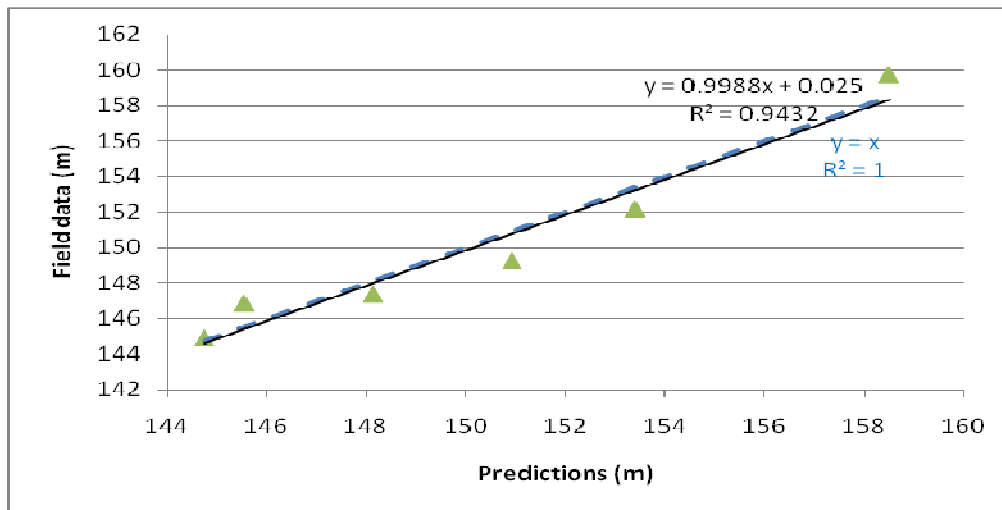


Figure 11. Comparison of predicted and measured maximum water levels of the 100 year flood for the main channel. Blue dashed line represents 1:1 compliance with monitoring data (ideal scenario) while the solid line demonstrates the observed compliance.

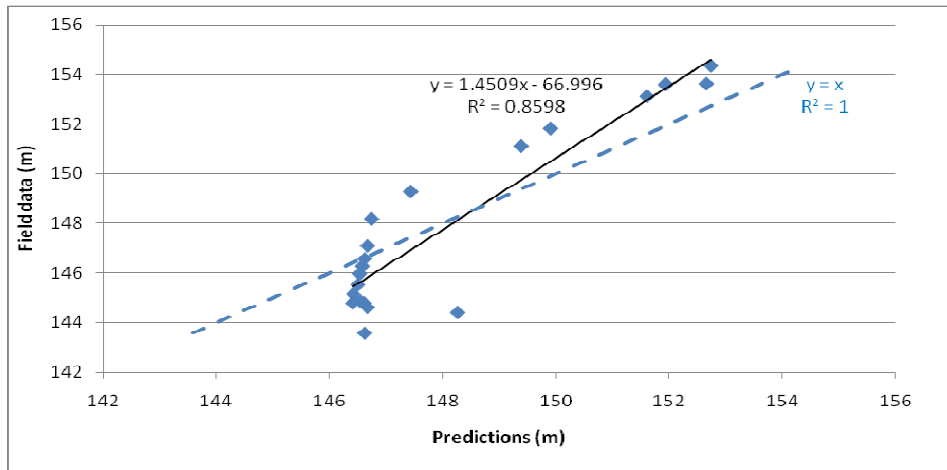


Figure 12. Comparison of predicted and measured maximum water levels of the 100 year flood for the floodplain. Blue dashed line demonstrates the ideal 1:1 result compliance, while the solid line represents the actual trend of compliance with Hydro2de predictions.

In addition, for assessing in numerical terms how well the calibrated model predictions match the field data, the Nash-Sutcliffe efficiency (E) was used for assessing the compliance of water levels (h) as defined by Equation 12. A perfect accuracy of a model would be described by a coefficient E value of 1. Table 5 summarises the calculated values of Nash-Sutcliffe efficiencies. All coefficients were approaching the value one, therefore, it can be said that the calibrated model results complied well with the field data. Steady state simulation produced results with the highest accuracy, followed by the unsteady simulation main channel and finally the unsteady flow floodplain results.

$$\text{Equation 12: } E = 1 - \frac{\sum (h_{obs} - h_{sim})^2}{\sum (h_{obs} - \bar{h}_{obs})^2}$$

Table 5. Nash-Sutcliffe efficiencies (E) for quantifying the model fit to field data.

Simulation		E
Steady state		0.999
100 year flood	Main channel	0.998
	Floodplain	0.997

### 3.1.2. Hydro2de comparison with calibrated HEC-RAS results

Donau Consult (2006) carried out and calibrated a number of flow simulations with various discharges in 1-D hydraulic model HEC-RAS. The study analysed the Danube reach from 1920.8 to 1868.75 river km with a cross-section of bed topography taken after every 200 m. The study ignored all floodplain flows, while any inflow to and outflow from major side arms was represented by a set of adjoining tributaries to the main channel. Therefore, only the main channel estimates of the current study could be compared with HEC-RAS results. For the unsteady flow simulations, the maximum predicted water levels and their equivalent velocities were

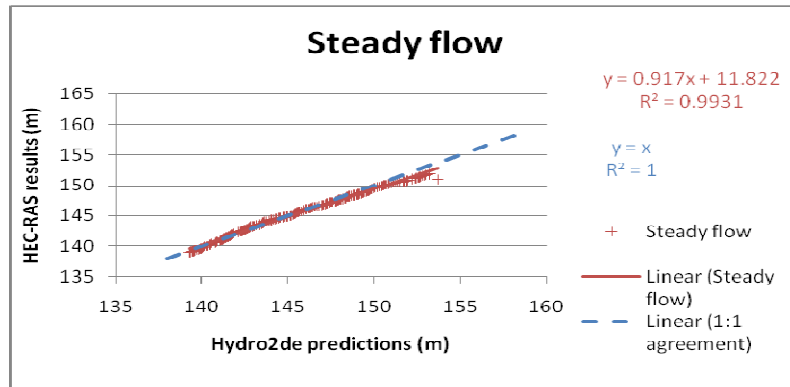
compared. Hence for comparison with HEC-RAS data, the maximum water level values of the main channel were subtracted from Hydro2de results after every 200 m. For flow velocities, an average velocity was calculated for every 200 m by first estimating the proportional contribution of each main channel cell to the total discharge from the channel, thereafter, multiplying the proportion by the velocity of the cell and finally, adding up the proportional velocities of the whole main channel cross-section. It is important to bear in mind that the values extracted from Hydro2de study represent averages for a 50 m<sup>2</sup> cell, while HEC-RAS results are point values for each cross-section. Therefore, some differences in the results are to be expected.

Figures 13 and 14 describe Hydro2de compliance with the HEC-RAS study results in terms of water levels and flow velocities respectively. The flow depths complied relatively well with HEC-RAS predictions while producing slope and  $r^2$  values near the ideal values one. As the regression lines produced a good fit with the 1:1 agreement, it can be said that the relatively large intercept values were produced due to the slight deviation of slope from 1, similarly to the steady state flow simulation.

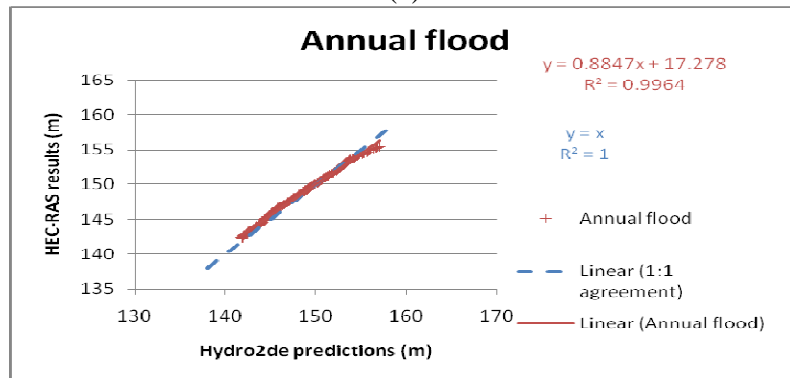
On the contrary, flow velocities demonstrated large fluctuations in terms of compliance with HEC-RAS data (Fig. 14). Although, all of the results centred around the 1:1 agreement trend line, i.e. Hydro2de velocities were at the same magnitude as HEC-RAS results, no real trend occurred for compliance as can be seen from the slope of the drawn regression lines. The scatter around the trend lines illustrates the inaccuracy/ inconsistent variation of the Hydro2de predictions while compared with HEC-RAS results which could be caused by both inaccuracies in HEC-RAS results and imprecise estimates of the Hydro2de model. Essentially, the calculated flow velocities are a function of input discharge, bed topography (shape, gradient) and the roughness of the area. As the results of HEC-RAS were calibrated to match monitored velocities and equivalent input discharges were used for both models, the differences in results were likely to be caused by either the inaccurate input data of Hydro2de (the applied bed topography and roughness coefficients) and/or the predictive ability of the model to calculate the variable.

It is important to note that the HEC-RAS study used a different set of bed topography from the Hydro2de model and a spatially variable roughness coefficient within the main channel. Papanicolaou (Thanos) *et al.* (2011) demonstrated that the accuracy of flow velocities predicted by a 2-D model can be significantly improved if roughness coefficients and eddy viscosities are spatially varied. For the purposes of this study, both of these variables were kept constant for the main channel. Moreover, a number of studies have demonstrated the dependence of flow velocities on the specification of bed topography due to its effect on flow routing and the inundation pattern (Lewin and Hughes, 1980; Nicholas and Walling, 1997; Nicholas and McLelland, 2004). Similarly, Nicholas (2003) demonstrated the lack of capability of the Hydro2de model to accurately depict naturally occurring fluctuations in flow velocities.

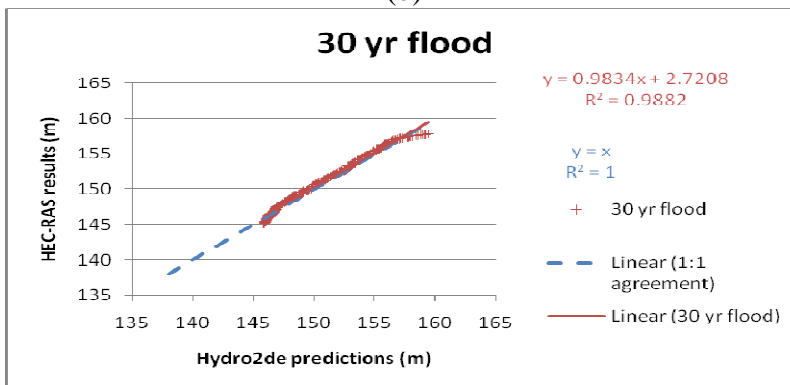
In addition, the predictions of flow velocities by Hydro2de were not calibrated as no field data was available for the process. Therefore, the comparison against calibrated results produced by HEC-RAS gives an indication of the Hydro2de's predictive capability for estimating flow velocities. As both, flow velocities and water levels, are necessary for calculating outflow discharge, which is the ultimate purpose of applying Hydro2de in this study, the results of the calculations will have to be treated with cautiousness while keeping in mind the conclusions of this comparison.



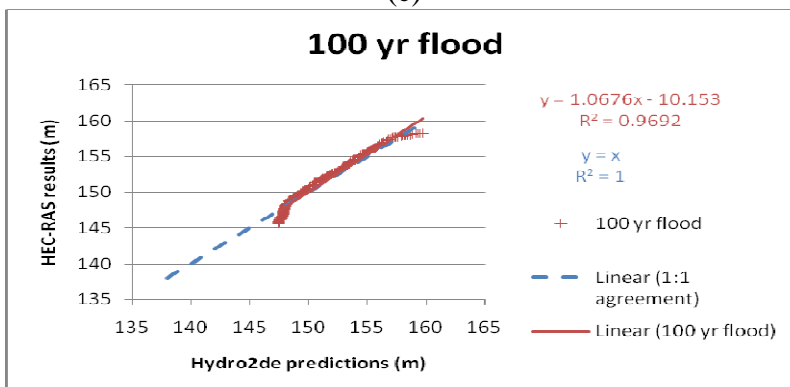
(a)



(b)



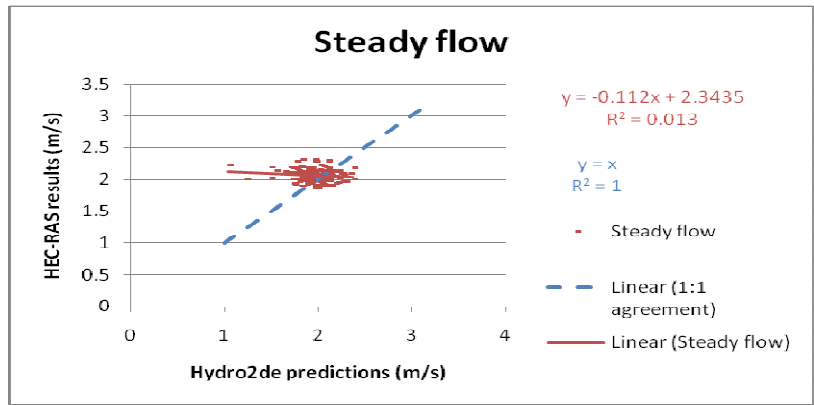
(c)



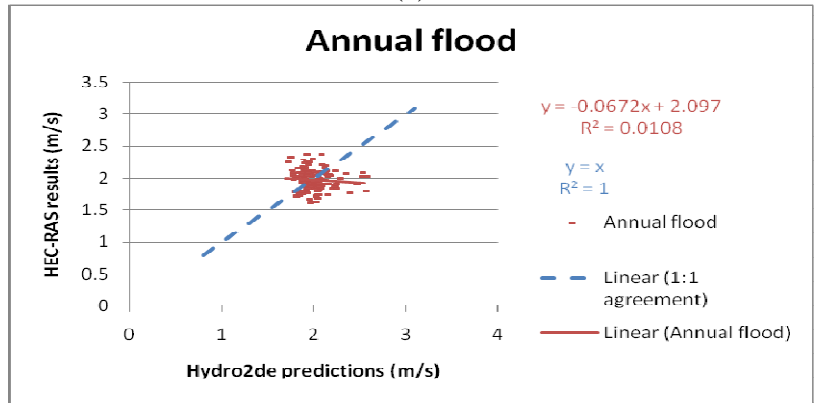
(d)

Figure 13. HEC-RAS and Hydro2de comparison of predicted water levels for the steady state (a), annual (b), 30- year (c) and 100-year flood events (d).

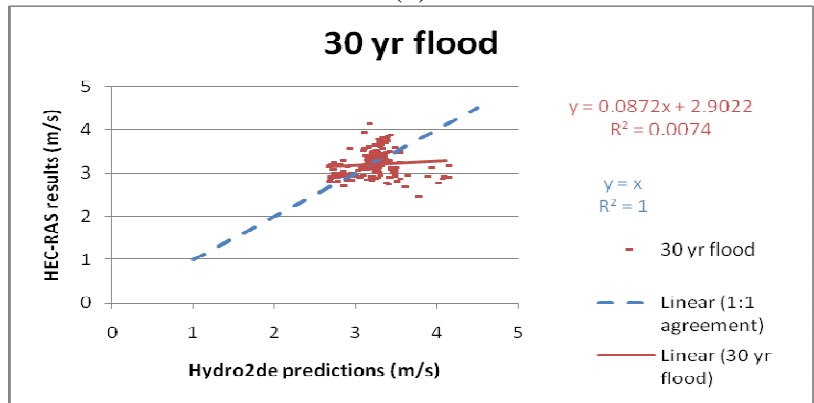




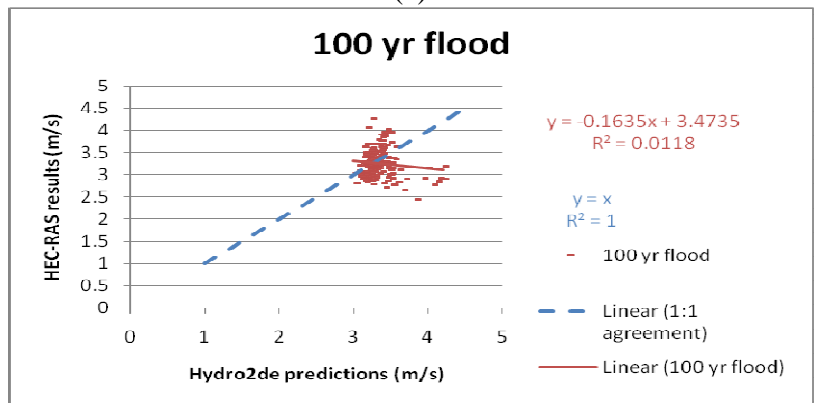
(a)



(b)



(c)



(d)

Figure 14. HEC-RAS and Hydro2de comparison of predicted flow velocities for steady state (a), annual (b), 30-year (c) and 100-year flood event (d).

## 3.2. Results of the modified non-linear reservoir method

### 3.2.1. Present flood retention capacity

The results of modelling to characterize the flood retention capacity of the Donau-Auen National Park in physical terms have been listed in Table 6 for the total study area and no-floodplain-flow scenarios. In addition, a difference in the retained water volumes of the two scenarios is included to represent the stored flood water volumes that could be solely accounted for the floodplains. A graphical representation of predicted flood extents and maximum flow depths is provided in Figure 15.

The volume of water stored across the total floodplain area for the annual flood was equivalent to 37% of inflow, while only 2% of the incoming flood waters was stored for the 30-year and 100-year flood events across the total study area. However, for the highest magnitude flood event modelled, the total study area stored up to 207 million  $m^3$  of flood waters which is equivalent to approximately  $658 \text{ l/m}^2$ . The contribution of the main channel flood retention capacity to the total ability of the study area to retain flood waters was minimal, i.e. equivalent to 0.03-0.06% of the total volume of retained flood water. Thus, the majority of flood waters were retained by the floodplains as can be evidenced from  $dV$  values in Table 6.

Moreover, the study showed that after an annual, 30 year or 100 year flood event, it would take around 5, 14 or 20 days respectively for the water levels to drop back to their averages and for the flood waters to exit the floodplain, assuming a steady inflow after the flood event that is equivalent to the average water levels of the Danube. The no-floodplain-flow scenario demonstrated how long it will take for one flood event to pass through the main channel, i.e. the time taken for the river stage to fall back to the steady state levels if no dewatering was to occur from the floodplains. Thus if no-floodplain-flow occurred, the retention times would be significantly shorter (2, 9 and 17 days respectively).

The flood peak velocity of all three flood events was approximately 2 km/h for the total study area scenario. The velocity increased for the no-floodplain-flow scenario by 2 - 4.5 times.

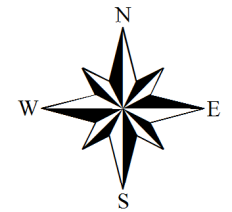
*Table 6. Summary of results for the present flood retention capacity. The following results are listed: retention volumes (V), residence times (T), average flood peak travelling velocities (v).*

	Annual flood	30 yr flood	100 yr flood
<b>Total flood retention capacity</b>	V= $1.24 \times 10^8 \text{ m}^3$ T= 122 h v= 2.17 km/h	V= $1.71 \times 10^8 \text{ m}^3$ T= 335 h v= 2.17 km/h	V= $2.07 \times 10^8 \text{ m}^3$ T= 488 h v= 2.30 km/h
<b>Flood retention capacity from the main channel (No-floodplain flow scenario)</b>	V= $7.16 \times 10^4 \text{ m}^3$ T= 47 h v= 7.81 km/h	V= $5.51 \times 10^4 \text{ m}^3$ T= 217 h v= 9.76 km/h	V= $7.16 \times 10^4 \text{ m}^3$ T= 415 h v= 4.88 km/h
<b>Water volume stored on floodplains</b>	$dV= 1.239 \times 10^8 \text{ m}^3$	$dV= 1.709 \times 10^8 \text{ m}^3$	$dV= 2.069 \times 10^8 \text{ m}^3$

Figure 15. Flood simulation results for the present scenario. Where (a) is 100-year flood event maximum flow depths, (b) 30-year flood event maximum flow depths, (c) annual flood event maximum flow depths.

**Depth**

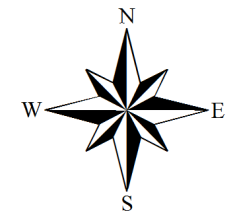
**Meters**



(a)

**Depth**

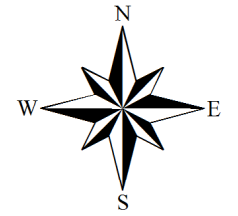
**Meters**



(b)

**Depth**

**Meters**



(c)

### 3.2.2. Past flood retention capacity

Table 7 lists the results of the physical flood retention quantification for the historical scenario. Estimated flow depths and flood extents have been provided in Figure 16.

According to the model predictions, the historical study area stored up to 24.6 mil.m<sup>3</sup> of flood waters during the highest magnitude flood event modelled which is the equivalent of 78 l/m<sup>2</sup>. Proportionally, 3.4%, 0.4% and 0.2% of the total inflow during the annual, 30 year and 100 year floods respectively were retained. The flood retention capacity of the anabranching main channel represented between 10.0% to 19.55% of the total storage capacity. Nevertheless, the majority of flood waters were still stored on the floodplains as can be evidenced from dV values on Table 7.

The retention times of the annual, 30 year and 100 year flood events averaged around 3, 10 and 15 days respectively for the total study area historical scenario, while if no floodplain flow occurred the retention times increased up to approximately 4, 11 and 17 days for the equivalent flood events.

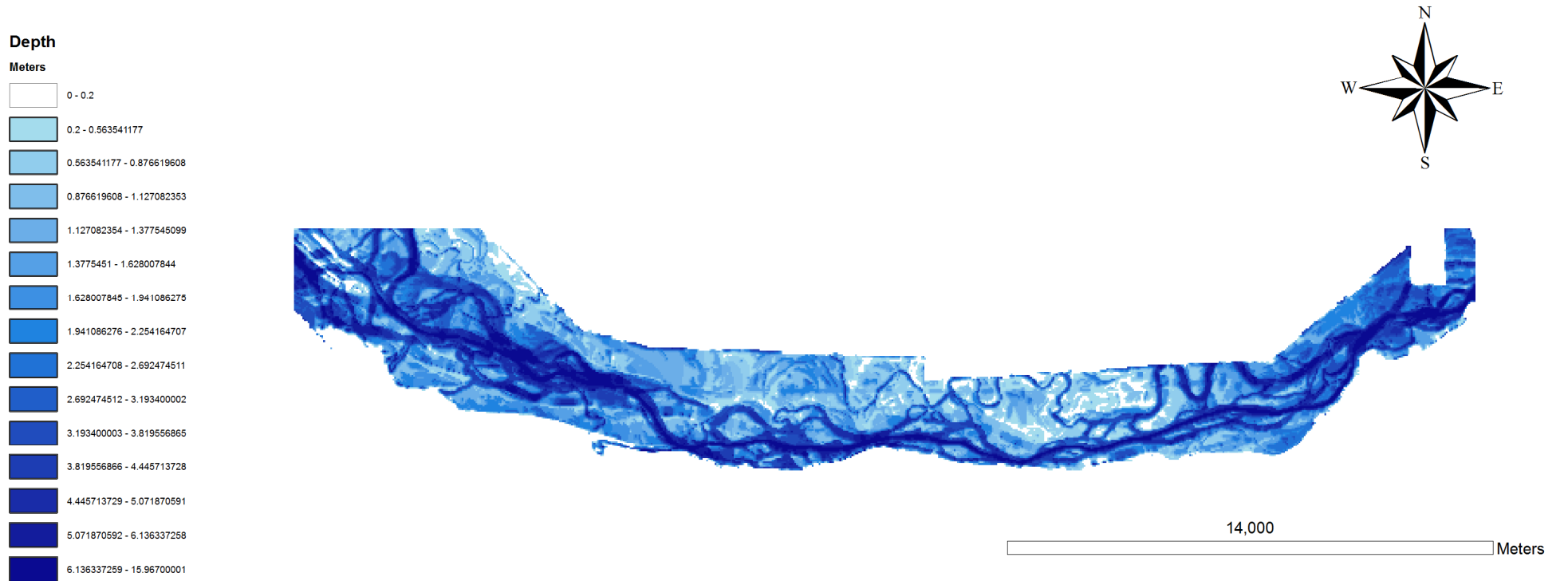
The flood peak velocity averaged around 3 km/h across the three flood events for the total study area simulations. A moderate increase to approximately 4 km/h occurred in the average velocity for the no-floodplain-flow scenario.

*Table 7. Summary of results for the estimated historical flood retention capacity. The following terms have been listed: retained volume of water (V), residence time (T), speed of the flood wave peak (v).*

	Annual flood	30 yr flood	100 yr flood
<b>Total flood retention capacity of the study area</b>	V= 1.15 x 10 <sup>7</sup> m <sup>3</sup> T= 79 h v= 2.60 km/h	V= 2.41 x 10 <sup>7</sup> m <sup>3</sup> T= 249 h v= 3.25 km/h	V= 2.46 x 10 <sup>7</sup> m <sup>3</sup> T= 364 h v= 2.79 km/h
<b>Flood retention capacity from the main channel (No-floodplain-flow scenario)</b>	V= 1.56 x 10 <sup>6</sup> m <sup>3</sup> T= 94 h v= 3.55 km/h	V= 2.43 x 10 <sup>6</sup> m <sup>3</sup> T= 262 h v= 4.33 km/h	V= 4.81 x 10 <sup>6</sup> m <sup>3</sup> T= 411 h v= 4.33 km/h
<b>Water volume stored on floodplains (Total study area-No-floodplain-flow scenario)</b>	dV= 9.94 x 10 <sup>6</sup> m <sup>3</sup>	dV= 2.17 x 10 <sup>7</sup> m <sup>3</sup>	dV= 1.98 x 10 <sup>7</sup> m <sup>3</sup>



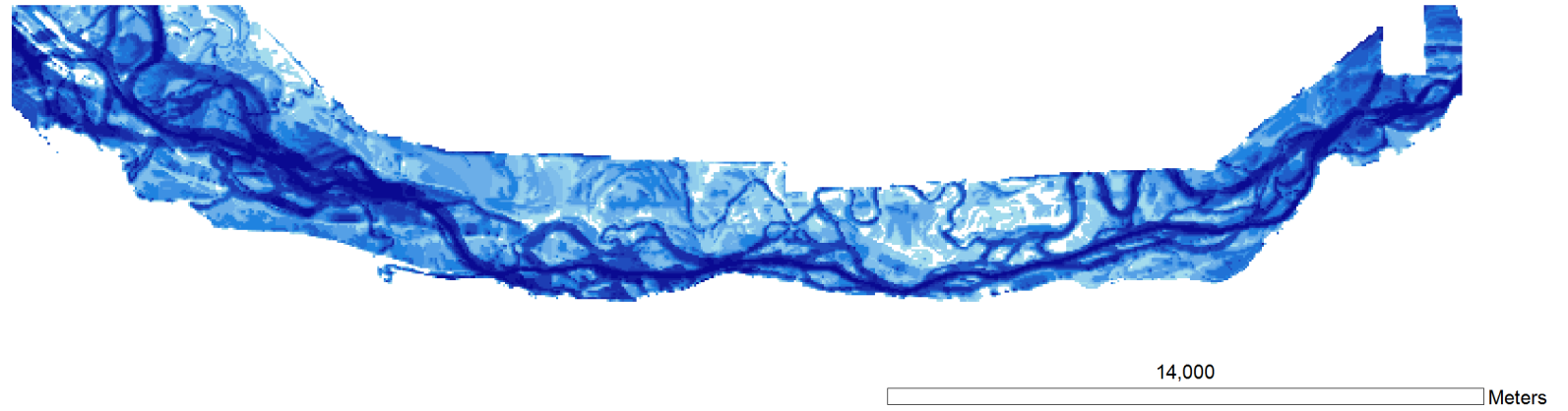
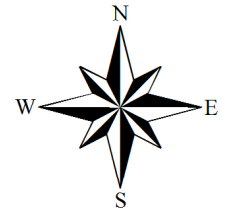
Figure 16. Flood simulation results for the past scenario. Where (a) is 100-year flood event maximum flow depths, (b) 30-year flood event maximum flow depths, (c) annual flood event maximum flow depths.



(a)

**Depth**

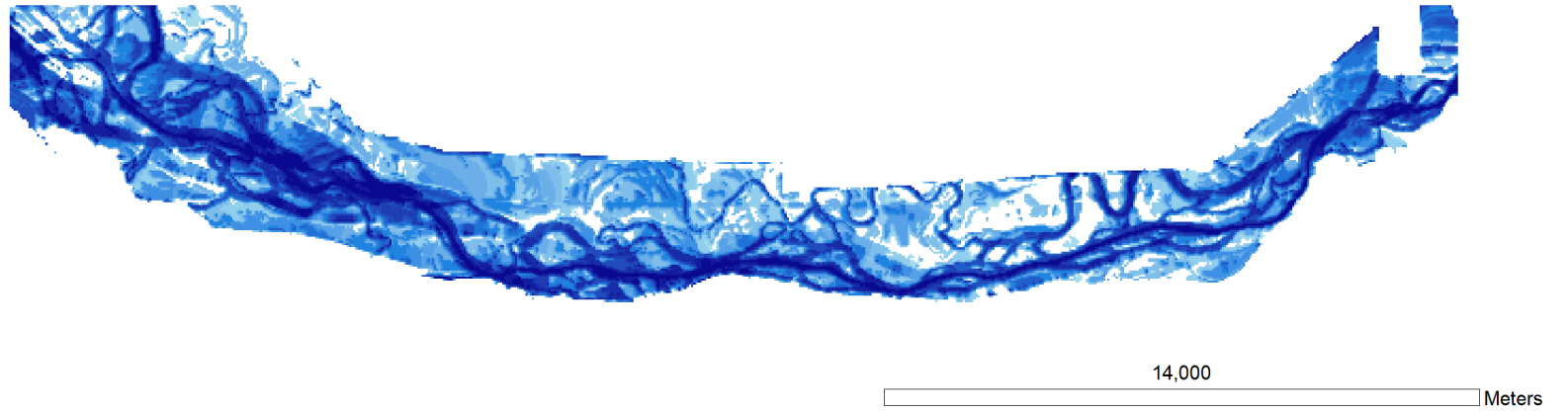
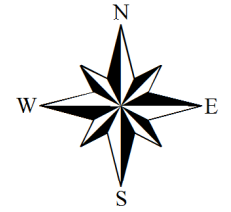
**Meters**



(b)

**Depth**

**Meters**



(c)

### 3.2.3. Future flood retention capacity

Estimated future flood retention capacity characteristics are listed in Table 8. Figure 17 provides a graphical representation of predicted flood extents and flow depths.

The maximum calculated volume of water stored by the total study area reached 178 mil.m<sup>3</sup> which is the equivalent of 570 l/m<sup>2</sup>. The main channel storage capacity formed 0.008%, 0.005% and 0.005% of the total retained flood water volume for the annual, 30 year and 100 year flood events respectively. Thus, the floodplains retained the majority of flood waters as can be observed from the dV values on Table 8.

In terms of residence times, it will take approximately 5, 13 and 18 days during the annual, 30 year and 100 year flood events for the water levels to lower back down to their average levels. On the other hand, for the no-floodplain-flow scenario the retention times of the flood events were the equivalents of 2, 9 and 13 days.

The average flood peak velocity was approximately 2 km/h for the total study area simulation across all flood events and 7 km/h for the no-floodplain-flow scenario.

*Table 8. Summary of results for the predicted future flood retention capacity. The following nomenclature was used: volume of water stored (V), residence time of the flood event (T), average velocity of the flood wave peak (v).*

	Annual flood	30 yr flood	100 yr flood
<b>Total flood retention capacity</b>	V= 1.01 x 10 <sup>8</sup> m <sup>3</sup> T= 128 h v= 2.30 km/h	V= 1.78 x 10 <sup>8</sup> m <sup>3</sup> T= 319 h v= 2.17 km/h	V= 1.78 x 10 <sup>8</sup> m <sup>3</sup> T= 433 h v= 1.86 km/h
<b>Flood retention capacity from the main channel (No-floodplain flow scenario)</b>	V= 7.93 x 10 <sup>4</sup> m <sup>3</sup> T= 50 h v= 7.81 km/h	V= 7.03 x 10 <sup>4</sup> m <sup>3</sup> T= 221 h v= 7.81 km/h	V= 7.07 x 10 <sup>4</sup> m <sup>3</sup> T= 323 h v= 4.88 km/h
<b>Water volume stored on floodplains (Total study area-No-floodplain-flow scenario)</b>	dV=1.009 x 10 <sup>8</sup> m <sup>3</sup>	dV=1.779 x 10 <sup>8</sup> m <sup>3</sup>	dV=1.779 x 10 <sup>8</sup> m <sup>3</sup>

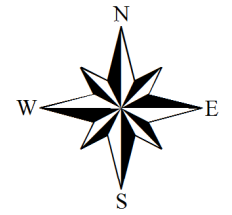
Figure 17. Flood simulation results for the future scenario. Where (a) is 100-year flood event maximum flow depths, (b) 30-year flood event maximum flow depths, (c) annual flood event maximum flow depths.



(a)

**Depth**

**Meters**

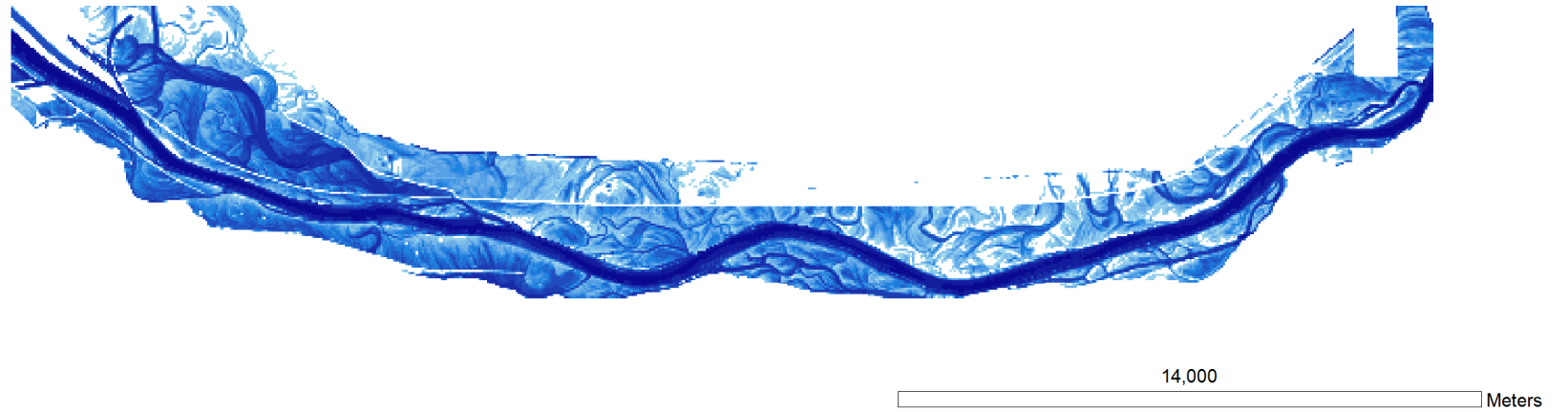
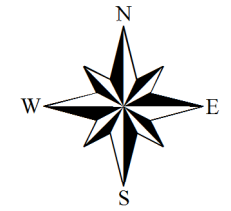


(b)



**Depth**

Meters



(c)

### 3.3. Monetary Value

A summary of results for the economic evaluation is provided in Table 9, which lists the monetary values of floodplains at different scenarios in terms of their produced cost savings for Bratislava's flood protection measures. The monetary values are also expressed in Euros per hectare of National Park per year. For example according to the substitute cost method results, it can be said that the current floodplain is valued at around 646,000 Euros at each year (i.e. there is no depreciation of the value over time). If the floodplains would cease to exist, Bratislava would need to invest another 646,000 Euros in flood protection and maintain the value of that investment from annual depreciation by yearly repairs.

Table 9. Summary of the monetary evaluation results.

	Total cost benefits for flood prevention (€/yr)	Benefits per National Park area per year (€ha <sup>-1</sup> yr <sup>-1</sup> )
<b>Present floodplains</b>	646,109	69
<b>Historical floodplains</b>	631,297	68
<b>Future floodplains</b>	646,107	69

## 4. Discussion of the estimated flood retention capacity

### 4.1. Present scenario

The stored water volumes in the study area increased non-linearly relative to the magnitude of flood event, suggesting an upper limit for the flood storage capacity of the study area, with the stored water volume approaching this capacity with increasing discharge. This can also be observed from the decreasing percentages with increasing flood magnitude, representing the relationship between retained water volumes and the total inflow. As the total inflow increased according to the magnitude of the flood event and the maximum retention capacity remained constant, it is only to be expected that a smaller percentage of the total inflow is stored.

The main channel flood retention capacity from the no-floodplain-flow scenario fluctuated between  $5.51 \times 10^4 \text{ m}^3$  to  $7.16 \times 10^4 \text{ m}^3$  with no consistent trend. It is to be expected that the main channel had a relatively constant capacity, however, fluctuations could have been produced as a result of inaccuracies in velocity modelling (see Section 3.1.2. and Fig.14) which is a component of the discharge function used in calculating the retained flood water volumes. However, the majority of flood retention in terms of stored water volumes (over 99.9%) is currently provided by the floodplain.

The residence times of flood waters were highly dependent on the duration of the flood event. For example, the calculated 122, 335 and 488 hours of residence for the annual, 30 year and 100 year flood waters respectively were equivalent to 39, 209 and 313 hours of inflow above the average water levels of the Danube.

The average flood peak velocity across the total study area remained relatively constant for the three flood events, i.e. around 2 km/h and more than tripled for the no-floodplain-flow scenario, suggesting that floodplains play an important role in decreasing the celerity of flood waves.

### 4.2. Past scenario

According to the model results, the historical scenario that used to represent the natural baseline of the area had a flood retention capacity of up to 182 mil.m<sup>3</sup> smaller than that of the present total study area and thus, the flood retention times were up to 124 h shorter (i.e. the change in T for the 100 year flood event). This can be explained by the fact that historically a much larger proportion of the floodplain area was governed by lotic conditions, hence transporting more water downstream and facilitating a better network of drainage from excess overbank flow. Thus, the model results imply that the return flows used to be more efficient. Although this may appear to be a negative effect in terms of flood risk reduction, it is important that floodplain storage is recovered in case a second flood wave rapidly follows the previous event.

The retention capacity of the main channel was comparatively larger than that in the present scenario, presumably due to the increased area of the anabranching main channels. In addition, the historical no-floodplain-flow scenario residence times were

higher than their equivalents in the present scenario (up to two times for the annual flood event) which could be accounted for the fact that the degree of meandering of the historical channel was much larger.

The average peak flow velocities were only slightly higher for the total study area simulations of the historical scenario (approximately 1 km/h) while compared to their present scenario equivalents. If a larger area of the river-floodplain system is actively taking part in transporting flow, it is only to be expected that the flood event is propagated over the area of the floodplains more quickly.

However, the velocity of the flood peak across the main channel was approximately two times smaller than its present scenario equivalent, presumably due to the higher degree of meandering. In addition, the difference between the total study area and no-floodplain-flow scenario velocities was smaller for the historical scenario than for the present. This suggests that historically the flood waves were more likely to be slowed down by the meanders of the river rather than as an effect of overbank flow.

### **4.3. Future scenario**

According to model predictions, the future flood storage capacity, along with calculated residence times, show an inclination to decrease, at least for the annual and 100-year flood event simulations, despite the small increase in the values of the 30-year flood event. This could be caused by the modifications made to the river bed due to the IREP objectives. As Tockner *et al.* (1998) described, the programme will enhance floodplain discharge and facilitate active flow in the side arm system, features that are more characteristic of the historical baseline of the area. However, as can be evidenced from the historical scenario, such increased lotic conditions actually decrease the flood storage capacity and retention time due to the fact that more water is returned rapidly to the main channel. On the other hand, the flood storage capacity of the main channel remained similar to the levels of the current scenario and the majority of flood waters (over 99.9%) were stored on the floodplains. In addition, no significant change in the average flood peak velocity across the three flood events occurred.

### **4.4. Monetary value**

As the physical flood retention capacity of the historical study area was likely to have been smaller, its monetary value in terms of providing flood protection benefits was estimated to be around 15,000 Euros less than the current value of the area. However, as the overall calculated changes in the future scenario's flood retention capacity were relatively small, the monetary value of the area did not change once the IREP objectives had been implemented according to the model results.

In order to provide a comparison of the monetary values calculated within this study with that for other wetlands, a few examples are listed in Table 10 for estimated wetland values for flood mitigation in different locations; these varied widely. For example the Charles River Basin wetlands (Thibodeau and Ostro, 1981) were estimated to have a monetary value per hectare per year of around 120 times greater

than that calculated for the Donau-Auen National Park. On the other hand, the estimated value per hectare per year of the National Park was close to the value of Whangamarino wetland in New Zealand (Kirkland, 1988). The large discrepancies could be produced by differences in methodology, assumptions made, size of the consumer group and thus, demand for the service, price levels in different countries and the functionality of the compared wetlands for flood retention. On the basis of this comparison, the need for a standardized methodology for assessing the monetary value of wetlands is apparent.

*Table 10. Comparison of wetland values in terms of produced flood benefits within literature.* The table was constructed after case studies presented in Schuyt and Brander, 2004. The currency conversion was carried out according to the USD/EUR rates on 14/08/2011.

Reference	Wetland location	Flood protection value in €ha <sup>1</sup> yr <sup>-1</sup>
<b>De Groot, 1992</b>	Dutch Wadden Sea, The Netherlands	491
<b>Emerton and Kekulandala, 2003</b>	Muthurajawela Wetland, Sri Lanka	1,152
<b>Kirkland, 1988</b>	Whangamarino wetland, North Island, New Zealand	41
<b>Leschine et al., 1997</b>	Scriber Creek Watershed, Lynnwood, Washington, US	453-680
	Springbrook Creek Watershed, Renton, Washington, US	2,390
<b>Ming et al., 2007</b>	Momoge National Nature Reserve, Jilin Province, China	4,002
<b>Thibodeau and Ostro, 1981</b>	Charles River Basin wetlands, Massachusetts, US	8,125
<b>n/a</b>	Donau-Auen National Park	69

It is also important to emphasize that the value of floodplains calculated in this study signifies only the value of flood protection services provided by the floodplains. The total economic value of the area is expected to be higher, as the floodplains provide many more ecosystem services beside flood storage.

#### **4.5. Model limitations**

The results of the model used in this study are subject to a number of limitations. Firstly, the study only accounted for flood storage effects that occur while overbank flow is distributed over the floodplains during high discharge and forms “pools” that remain on the floodplain even when the main channel water levels have lowered. Therefore, the study did not account for the effects of infiltration, aquifer storage or evapotranspiration. Further research would also be needed for quantifying how the infiltration rate has changed over time and how quickly the soils become saturated during a flood event. The exploration of these questions would however, require

resources not available for this study in terms of time and field work. As a result, the actual flood storage capacity of the study area is likely to be larger and the residence times of flood events shorter. Thus, the physical flood storage values reported here should be considered as the lower limit of flood retention capacity.

Secondly, the topographic data input file also covered some areas outside the official borders of the Donau-Auen National Park, thus the surface water retention calculated in this study is in practice larger than that for the National Park itself. However, this does not affect the economic value of the area for flood protection because the National Park facilitates the distribution of flow across the Danube valley and thus, maintains the hydrological connectivity of the floodplains and enables flood water storage of the area as a whole. If no overbank flow could access the National Park area, no value would be produced from the whole study region for flood protection.

Thirdly, the model accuracy is limited by the assumptions made for model construction. The velocity predictions proved to be relatively imprecise although in the right magnitude, no calibration against monitored discharges was made, relatively constant roughness coefficients and a single value for the turbulence coefficient were used. In addition, a simple proxy for the capital flood storage unit was adopted on the basis of previous investment. The historical and future scenarios are also only approximations of the real values due to the uncertainties that the modelling of past and future ecosystems involves. Thus, the constructed methodology needs further development for producing more accurate results. Nevertheless, the calculated flood retention values are likely to roughly describe the main characteristics of the floodplains in terms of flood mitigation.



## 5. Conclusion

To summarise, the study developed a methodology for calculating flood retention capacity of the Danube floodplains in the Donau-Auen National Park, Austria. For the physical quantification of the ecosystem service, Hydro2de, a two-dimensional hydrodynamic model was used to estimate the outflow hydrographs of three flood events with a recurrence interval of one, thirty and one hundred years. Thereafter, a modified non-linear reservoir model was applied to calculate the volumes of stored flood water during modelled flood events, their residence times and peak flood wave velocities. However in order to calculate the contribution of floodplains to the flood retention capacity of the total study area, a topography where no overbank flow occurs was constructed (i.e. no floodplain surface elevations were included within the data input file). This topography was applied to the annual, 30-year and 100-year flood event simulations and was assumed to represent the flood retention capacity of the main channel alone. Therefore, the difference between the flood storage volumes of simulations using a complete topography and only the main channel topography was calculated to represent the flood retention capacity of floodplains.

In addition, the same methodology was used to estimate the flood retention capacity of the area for both a past and a future scenario. The past and future estimates of the area were calculated on the basis of modified input files used to represent the likely historical and future conditions. For example, historical maps from the 18<sup>th</sup> century were used to identify the past location and distribution of the Danube channels while for the future scenario, the input files were modified according to the objectives of a restoration programme, planned to be carried out in the near future (the Integrated River Engineering Programme).

The physical quantification estimated a current maximum flood storage of 207 million m<sup>3</sup> by the total study area for the case of the 100-year flood event which is the equivalent of 2% of the total inflow during the event. Over 99.9% of the stored water volume was accommodated by the floodplains. The residence times of flood waters depended strongly on the actual length of the event and ranged from 5 to 20 days between the three modelled flood events. The peak flood wave velocity demonstrated a relatively constant celerity of 2 km/h.

The historical scenario indicated that in the past the flood retention capacity of the area used to be smaller by up to 182 million m<sup>3</sup> for the case of the 100-year flood event, as a larger proportion of the study area was actively involved in transporting flood waters downstream. Therefore, the residence times of flood events also used to be shorter and average flood peak velocities higher.

The future scenario predicted a small decrease in the stored flood water volumes and residence times as the restoration programme enhances discharge from floodplains due to a better hydrological connectivity. However, no significant change in the average flood peak velocity was estimated. While the results of the model imply that the restoration of the floodplain may reduce the flood retention capacity of the area, it is important to note that the programme does recover historic conditions and enhances biodiversity. In addition, the restoration programme is likely to ensure a better balance between flood storage and floodplain dewatering by return flows, which then recovers the potential for storage in an immediately following flood event.

The economic value of the flood retention capacity was calculated by a substitute cost method with the population of Bratislava as the target consumer group. The current value of the ecosystem service was estimated to be approximately 646,000 Euros or 69 Euros per ha per year. The evaluation concluded that the historical value used to be around 15,000 Euros less or 68 Euros per ha per year. The predicted future changes in the physical flood retention capacity did not produce any significant change in the monetary value of the area.

The accuracy of the methodology used in this study is limited by a number of assumptions and simplifications made. Thus, the results could be improved if the effects of soil infiltration and evapotranspiration were included along with more variable roughness and turbulence coefficients. Moreover for a better calibration of the model, spatially distributed field data on discharge values during different flood events should be recorded. Despite the high potential for model development, the results of the study provide a useful characterisation of the dominant features of flood retention provisioning by the Danube floodplains in Austria and the methodology employed may have a wider value.

## References

- Arcement, G. J. and Schneider, V.R. (1989) Guide for selecting Manning's roughness coefficients for natural channels and flood plains. *US Geological Survey Water Supply Paper 2339*. 38p.
- Barbier, E.B., Acreman, M. and Knowler, D. (1997) Economic valuation of wetlands: A guide for policy makers. Ramsar Convention Bureau. Gland, Switzerland.
- Beffa, C. and Connell, R.J. (2001) Two-dimensional flood plain flow. I: Model description. *Journal of Hydrologic Engineering*. 6(5): 397-405.
- Bouma, J.J., Francois, D. and Troch, P. (2005) Risk assessment and water management. *Environmental Modelling and Software*. 20: 141-151.
- Casas, A., Lane, S.N., Yu, D. and Benito, G. (2010) A method for parameterising roughness and topographic sub-grid scale effects in hydraulic modelling from LiDAR data. *Hydrology and Earth System Sciences*. 14 (8): 1567-1579.
- Cierjacks, A., Kleinschmit, B., Babinsky, M., Kleinschroth, F., Markert, A., Menzel, M., Ziechmann, U., Schiller, T., Graf, M., Lang., F. (2010) Carbon stocks of soil and vegetation on Danubian floodplains. *Journal of Plant Nutrition and Soil Science*. 173: 644-653.
- Cobby, D.M., Mason, D.C. and Davenport, I.J. (2001) Image processing of airborne scanning laser altimetry data for improved river flood modelling. *Journal of Photogrammetry and Remote Sensing*. 56: 121-138.
- Connell, R.J., Beffa, C., Painter, D.J. (1998) Comparison of observations by flood plain residents with results from a two-dimensional flood plain model: Waihao River, New Zealand. *Journal of Hydrology*. 37: 55-79.
- Connell, R.J., Painter, D.J. and Beffa, C. (2001) Two-dimensional flood plain flow. II: Model validation. *Journal of Hydrologic Engineering*. 6 (5): 406-415.
- De Groot, R.S. (1992) *Functions of Nature: evaluation of nature in environmental planning, management and decision-making*. Wolters Noordhoff BV. Groningen. Netherlands, 345 pp.
- Donau Consult (2006) Flussbauliches Gesamtprojekt Donau Östlich Von Wien: Hydraulische Berechnungen. *Via donau*.
- Emerton, L. and Kekulandala, L.D.C.B. (2003) Assessment of the economic value of Muthurajawela wetland. *Occasional Papers of IUCN Sri Lanka*. No.4
- Flavelle, P. (1992) A quantitative measure of model validation and its potential use for regulatory purposes. *Advances in Water Resources*. 19: 5-13.

Fukuoka, S. and Watanabe, A. (2002) Estimating channel storage and discharge hydrographs of flooding. *5th International Conference on Hydro -Science & -Engineering*. Warsaw, Poland.

Hirnerova, D. and Sabo, J. (2010) Project: Bratislava Flood Protection. *Conference on the European Union Strategy for the Danube Region: Transport, energy and environmental issues*. Vienna and Bratislava, April 2010.

Hohensinner, S., Jungwirth, M., Muhar, S. and Habersack, H. (2005) Historical analyses: A foundation for developing and evaluating river-type specific restoration programs. *International Journal of River Basin Management*.

Hohensinner, S. and Drescher, A. (2008) Historical change of European floodplains: the Danube River in Austria. In: *The Floodplain Forests of Temperate Zone of Europe*. Eds. Klimo, E., Hager, H., Matic, S., Anic, I. and Kulhavy, J. Lesnická práce, Prague.

ICPDR (International Commission for the Protection of the Danube River) (2010) Report on Achievements in Flood Protection in the Danube River Basin. [www.icpdr.org/icpdr-files/15473](http://www.icpdr.org/icpdr-files/15473) [Accessed 5 August 2011]

Keckeis, H. and Schiemer, F. (2002) Understanding Conservation Issues of the Danube River. *Fishery Science: The unique contribution of early life stages*. Eds. Fuiman, L.A. and Werner, R.G. Blackwell Science. pp. 272-288.

King, D.M. and Mazzotta, M.J. (2000) Damage Cost Avoided, Replacement Cost, and Substitute Cost Methods. *Ecosystem Valuation*. [http://www.ecosystemvaluation.org/cost\\_avoided.htm](http://www.ecosystemvaluation.org/cost_avoided.htm) [Accessed 19 July 2011]

Kirkland, W.T. (1988) Preserving the Whangamarino wetland – an application of the contingent valuation method, Master's Thesis, Massey University, New Zealand. Cited in Schuyt, K. and Brander, L. (2004)

Kotze, D.C. (2000) The Contribution of Wetlands to the Attenuation of Floods. *Mondi Wetlands Programme*, October 2000.

Lane, S.N, Hardy, R.J., Ferguson, R.J. and Parson, D.R. (2005) A framework for model verification and validation of CFD schemes in natural open channel flows. In *Computational Fluid Dynamics: Applications in Environmental Hydraulics*. Eds. P.D. Bates, S.N. Lane and R.I. Ferguson. John Wiley & Sons Ltd, England.

Leschine, T.M., Wellman, K.F. and Green, T.H. (1997) The Economic Value of Wetlands: Wetlands' Role in Flood Protection in Western Washington. The Department of Ecology, State of Washington. <http://www.ecy.wa.gov/biblio/97100.html> [Accessed 4 August 2011]

Lewin, J. and Hughes, D. (1980) Welsh floodplain studies II. Application of a qualitative inundation model. *Journal of Hydrology*. 46: 35–49.

Liptak, R. (2007) Flood protection in Slovakia and the Slovak Water Management Enterprise, s.e. *The INBO 7<sup>th</sup> World General Assembly*. June, Debrecen, Hungary.

[www.riob.org/IMG/pdf/LIPTAK\\_Slovakia\\_Floods\\_andSWE.pdf](http://www.riob.org/IMG/pdf/LIPTAK_Slovakia_Floods_andSWE.pdf) [Accessed 5 August 2011]

Millennium Ecosystem Assessment (2005) *Current State and Trends Assessment: Inland Water Systems*. Island Press, Washington DC.

Ming, J., Xian-guo, L., Lin-shu, X., Li-juan, C. and Shouzheng, T. (2007) Flood mitigation benefit of wetland soil – A case study in Momoge National Nature Reserve in China. *Ecological Economics*. 61: 217-223.

Mirosław-Swiątek, D., Okruszko, T., Chormanski, J. (2003) Natural floodplain storage capacity modelling approach. *International Conference "Towards natural flood reduction strategies"*, Warsaw, 6-13 September 2003.

Mitkova, V., Pekarova, P., Miklaner, P. and Pekar, J. (2005) Analysis of flood propagation changes in the Kienstock–Bratislava reach of the Danube River. *Hydrological Sciences*. 50 (4): 655-668.

Mohilla, P. and Michlmayr, F. (1996) Atlas of the Danube river, Vienna: A History of River Training On Maps and Plans of Four Centuries. Österreichischer Kunst und Kulturverlag Wien.

Nationalpark Donau-Auen GmbH (2011)  
<http://www.donauauen.at/?area=home&language=english> [Accessed 9 July 2011]

Nicholas, A.P. (2003) Investigation of spatially distributed braided river flows using a two-dimensional hydraulic model. *Earth Surface Processes and Landforms*. 28: 655-674.

Nicholas, A.P. (2005) Roughness parameterization in CFD modelling of gravel-bed rivers. In *Computational Fluid Dynamics: Applications in Environmental Hydraulics*. Eds. P.D. Bates, S.N. Lane and R.I. Ferguson. John Wiley & Sons Ltd, England.

Nicholas, A.P. and McLelland, S.J. (2004) Computational fluid dynamics modelling of three dimensional processes on natural river floodplains. *Journal of Hydraulic Research*. 42 (2): 131-143.

Nicholas, A.P. and Mitchell, C.A. (2003) Numerical simulation of overbank processes in topographically complex floodplain environments. *Hydrological Processes*. 17: 727-746.

Nicholas, A.P. and Walling, D.E. (1997) Modelling flood hydraulics and overbank deposition on river floodplains. *Earth Surface Processes and Landforms*. 22: 59–77.

Ogawa, H. and Male, J.W. (1986) Simulating the flood mitigation role of wetlands. *Journal of Water Resources Planning and Management*. 112: 114-128.

Papanicolaou (Thanos), A.N., Elhakeem, M. and Wardman, B. (2011) Calibration and verification of a 2D hydrodynamic model for simulating flow around

emergent bendway weir structures. *Journal of Hydraulic Engineering*. 137 (1): 75-89.

Pithart, D., Prach, K., Francirkova, T. (2003) Functional river floodplains as the best flood protection: the Luznice River, Czech Republic, experience from August 2002 flooding. International Conference Towards Natural Flood Reduction Strategies, Warsaw.

Reckendorfer, W., Schmalfluss, R., Baumgartner, C., Habersack, H., Hohensinner, S., Jungwirth, M. and Schiemer, F. (2005) The Integrated River Engineering Project for the free-flowing Danube in the Austrian Alluvial Zone National Park: contradictory goals and mutual solutions. *Large Rivers*. 15: 1-4.

Roache, P.J. (1994) Perspective: A method for uniform reporting of grid refinement studies. *Journal of Fluids Engineering*. 116: 405-413.

Roache, P.J. (1997) Quantification of uncertainty in computational fluid dynamics. *Annual Reviews in Fluid Mechanics*. 29: 123-160.

Roe, P. L. (1981) Approximate Riemann solvers, parameter vectors and difference schemes. *Journal of Computational Physics*. 43: 357-372.7

Sabacek, P. (2011) Project of Bratislava flood protection is officially completed. *Slovensky rozhlas*. <http://www.rozhlas.sk/radio-international-en/news/Project-of-Bratislava-flood-protection-is-officially-completed?l=2&i=480&p=6> [Accessed 5 August 2011]

Sartor, J.F. (2005) Flood water retention by riverine and terrestrial forests. *Proceedings of the 2005 Watershed Management Conference*, Williamsburg.

Schiemer, F., Baumgartner, C. and Tockner, K. (1999) Restoration of floodplain rivers: The Danube Restoration Project. *Regulated rivers: research and management*. 15: 231-244.

Schuyt, K. and Brander, L. (2004) The economic values of the world's wetlands. Living Waters: conserving the source of life. WWF [www.panda.org/downloads/freshwater/wetlandsbrochurefinal.pdf](http://www.panda.org/downloads/freshwater/wetlandsbrochurefinal.pdf) [Accessed 19 July 2011]

Schwarz, U. (2010) Assessment of the restoration potential along the Danube and main tributaries. Working paper for the Danube River Basin. WWF International.

Straatsma, M.W. and Baptist, M.J. (2008) Floodplain roughness parameterization using airborne laser scanning and spectral remote sensing. *Remote Sensing of Environment*. 112 (3): 1062-1080.

Szolgay, J. and Danacova, M. (2008) Detection of changes in the flood celerity by multilinear routing on the Morava River. *XXIVth Conference of the Danubian Countries on the Hydrological Forecasting and Hydrological Bases of Water Management*. Bled, Slovenia.



- Thibodeau, F.R. and Ostro, B.D. (1981) An economic analysis of wetland protection. *Journal of Environmental Management*. 12: 19-30.
- Tockner, K., Schiemer, F. and Ward, J.V. (1998) Conservation by restoration: the management concept for a river-floodplain system on the Danube River in Austria. *Aquatic Conservation: Marine and Freshwater Ecosystems*. 8: 71-86.
- Tockner, K. and Schiemer, F. (1997) Ecological aspects of the restoration strategy for a river-floodplain system on the Danube River in Austria. *Global Ecology and Biogeography Letters*. 6: 321-329.
- Valentova, J., Valenta, P., Weyskrabova, L. (2010) Assessing the retention capacity of a floodplain using a 2D numerical model. *Journal of Hydrology and Hydromechanics*. 58 (4): 221-232.
- Van Leer, B. (1977) Towards the ultimate conservative difference scheme. A new approach to numerical convection. *Journal of Computational Physics*. 23: 276–299.
- Via donau (1996) Characteristic water levels of the Danube.  
[http://www.donauschiffahrt.info/en/facts\\_figures/the\\_danube\\_as\\_a\\_major\\_route\\_of\\_transport/navigability/](http://www.donauschiffahrt.info/en/facts_figures/the_danube_as_a_major_route_of_transport/navigability/) [Accessed on 18 March 2011]
- Wilson, C.A.M.E., Stoesser, T., and Bates, P. (2005) Modelling of open channel flow through vegetation. In *Computational Fluid Dynamics: Applications in Environmental Hydraulics*. Eds. P.D. Bates, S.N. Lane and R.I. Ferguson. John Wiley & Sons Ltd, England.

## Appendix A

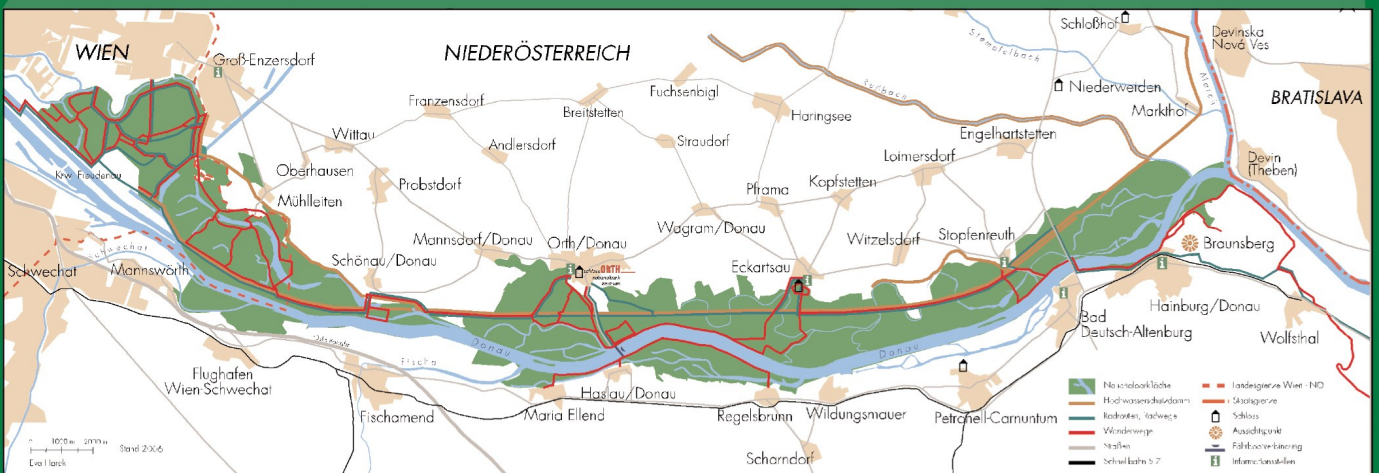
Table 1. Percentage change in flow depth values with varying resolution. E.g. Perc 15-20 signifies the percentage difference of 15 m resolution depth values from the 20 m resolution results. Negative values represent differences where the estimates of the 20 m resolution simulation were higher than those of the 15 m resolution.

	Mean %	St dev %	Min %	Max%	Median%	Outlier %
Perc 15-20	0.2	-175.4	-100	40200	-2.12	11.34
Perc 15-25	5.9	-481.5	-100	80400	-2.76	11.24
Perc 15-30	10.79	-576.29	-100	81900	-3.85	8.80
Perc15-40	30.74	-1180	-100	135200	-6.92	10.22
Perc15-50	31.05	-1366.7	-100	186700	-11.86	11.28
Perc15-60	35.61	-1097.8	-100	90400	-15.05	11.45
Perc15-70	24.13	-742.9	-100	67500	-20.88	9.65
Perc15-80	22.00	-630.3	-100	35340	-27.41	9.34
Perc15-90	22.78	-766.9	-100	44120	-27.27	8.80
Perc15-100	20.40	-865.0	-100	61500	-28.57	8.26

Table 2. A summary of percentage changes in velocities for different resolution topographies. For example, V\_Perc\_15-20 signifies percentage difference of 15 m resolution from 20 m resolution results.

	Mean %	St dev %	Min %	Max %	Median %	Outlier %
V_Perc 15-20	47.98	-618.15	-100	134400	0.67	16.27
V_Perc 15-25	128.62	-1272.7	-100	173500	5.08	16.19
V_Perc 15-30	216.08	-1661.9	-100	155800	5.77	15.68
V_perc15-40	289.07	-2587	-100	181000	4.08	15.45
V_perc15-50	279.03	-2028.4	-100	160700	-0.68	13.78
V_perc15-60	293.53	-1834.4	-100	65300	-1.81	13.84
V_perc15-70	326.84	-2150.4	-100	67900	-4.46	13.81
V_perc15-80	305.33	-1933.7	-100	92600	-8.26	13.54
V_perc15-90	288.78	-2013.4	-100	132400	-9.48	13.15
V_perc15-100	325.09	-2783.4	-100	103800	-8.75	12.53

- Herausgeber: Nationalpark Donau-Auen GmbH
- Titelbild: A. Tishler
- Für den Inhalt sind die Autoren verantwortlich
- Für den privaten Gebrauch beliebig zu vervielfältigen
- Nutzungsrechte der wissenschaftlichen Daten verbleiben beim Rechtsinhaber
- Als pdf-Datei direkt zu beziehen unter [www.donauauen.at](http://www.donauauen.at)
- Bei Vervielfältigung sind Titel und Herausgeber zu nennen / any reproduction in full or part of this publication must mention the title and credit the publisher as the copyright owner:  
© Nationalpark Donau-Auen GmbH
- Zitiervorschlag: TISHLER, A. (2016) An Evaluation of Flood Retention Capacity by the Danube Floodplains in Austria. Wissenschaftliche Reihe Nationalpark Donau-Auen, Heft 54



# ZOBODAT - [www.zobodat.at](http://www.zobodat.at)

Zoologisch-Botanische Datenbank/Zoological-Botanical Database

Digitale Literatur/Digital Literature

Zeitschrift/Journal: [Nationalpark Donauauen - Wissenschaftliche Reihe](#)

Jahr/Year: 2016

Band/Volume: [54](#)

Autor(en)/Author(s): Tischler Astrid

Artikel/Article: [An Evaluation of Flood Retention Capacity by the Danube Floodplains in Austria 1-65](#)